EJN fens European Journal of Neuroscience

European Journal of Neuroscience, Vol. 37, pp. 80–95, 2013 doi:10.1111/ejn.12024

NEUROSYSTEMS

Effects of the α_2-adrenergic receptor agonist dexmedetomidine on neural, vascular and BOLD fMRI responses in the somatosensory cortex

Mitsuhiro Fukuda,[1] Alberto L. Vazquez,[1] Xiaopeng Zong[1] and Seong-Gi Kim[1,2]
[1]Neuroimaging Laboratory, Department of Radiology, University of Pittsburgh, Pittsburgh, PA, USA
[2]Department of Neurobiology, University of Pittsburgh, Pittsburgh, PA, USA

Keywords: blood oxygenation level-dependent, cerebral blood volume, functional connectivity, medetomidine, rat

Abstract

This article describes the effects of dexmedetomidine (DEX) – the active ingredient of medetomidine, which is the latest popular sedative for functional magnetic resonance imaging (fMRI) in rodents – on multiple unit activity, local field potential (LFP), cerebral blood flow (CBF), pial vessel diameter [indicative of cerebral blood volume (CBV)], and blood oxygenation level-dependent (BOLD) fMRI. These measurements were obtained from the rat somatosensory cortex during 10 s of forepaw stimulation. We found that the continuous intravascular systemic infusion of DEX (50 μg/kg/h, doses typically used in fMRI studies) caused epileptic activities, and that supplemental isoflurane (ISO) administration of ~0.3% helped to suppress the development of epileptic activities and maintained robust neuronal and hemodynamic responses for up to 3 h. Supplemental administration of N_2O in addition to DEX nearly abolished hemodynamic responses even if neuronal activity remained. Under DEX + ISO anesthesia, spike firing rate and the delta power of LFP increased, whereas beta and gamma power decreased, as compared with ISO-only anesthesia. DEX administration caused pial arteries and veins to constrict nearly equally, resulting in decreases in baseline CBF and CBV. Evoked LFP and CBF responses to forepaw stimulation were largest at a frequency of 8–10 Hz, and a non-linear relationship was observed. Similarly, BOLD fMRI responses measured at 9.4 T were largest at a frequency of 10 Hz. Both pial arteries and veins dilated rapidly (artery, 32.2%; vein, 5.8%), and venous diameter returned to baseline slower than arterial diameter. These results will be useful for designing, conducting and interpreting fMRI experiments under DEX sedation.

Introduction

Anesthesia is commonly used in functional brain imaging studies that investigate a wide variety of neuroscience research questions, including neurovascular relationships, pain mechanisms, consciousness, longitudinal functional development, and reorganisation. Imaging studies are often performed in immobilised animals to avoid motion artefacts. As immobilisation without stress is not often possible, particularly for relatively long recording sessions in alert animals, the use of anesthesia is beneficial. Anesthesia, however, can modify neuronal and hemodynamic activity (Berwick *et al.*, 2002; Martin *et al.*, 2006). Thus, it is critical to understand the impact of anesthesia on neuronal and hemodynamic responses.

Two anesthetic agents, isoflurane (ISO) and medetomidine (MED), are often used for functional magnetic resonance imaging (fMRI) experiments, because of their ability to enable longitudinal studies. Our group previously explored the impact of ISO anesthesia on neurovascular responses in the rat forepaw model (Masamoto *et al.*, 2007, 2009; Kim *et al.*, 2010). ISO at approximately one minimum alveolar concentration (1.38%) (White *et al.*, 1974) provides a stable physiological situation for experiments lasting for > 6 h. However, ISO strongly suppresses neuronal activity (Banoub *et al.*, 2003) and dilates blood vessels (Iida *et al.*, 1998), thus reducing evoked hemodynamic responses. Thus, the use of ISO for fMRI studies has been limited. Meanwhile, MED has recently become popular for rodent fMRI studies over various brain regions, including the brain stem, hippocampus, basal ganglia, and neocortex (Van Camp *et al.*, 2006; Weber *et al.*, 2006; Zhao *et al.*, 2008; Angenstein *et al.*, 2010), largely because MED yields robust hemodynamic responses; however, this effect lasts for < 3 h (Pawela *et al.*, 2009). Despite the popularity of MED, its effects on physiological parameters, such as cerebral blood flow (CBF), cerebral blood volume (CBV), and neuronal activity, at the doses typically used in fMRI studies (100 μg/kg/h) have not been established.

The pharmacological effects of MED are attributed to its optical isomer, dexmedetomidine (DEX), and thus both MED and DEX exert the same physiological effects (Vickery & Maze, 1989; MacDonald *et al.*, 1991; Savola & Virtanen, 1991; Schmeling *et al.*, 1991). DEX is a highly selective α_2-adrenergic receptor agonist that crosses the blood–brain barrier. DEX produces sedation and analgesia dose-dependently, with a minimal effect on the respiratory system, despite the muscular relaxation that it causes (Doze *et al.*, 1989; Kalso *et al.*, 1991; Correa-Sales *et al.*, 1992; Guo *et al.*,

Correspondence: Mitsuhiro Fukuda, [2]McGowan Institute, as above.
E-mail: mif5@pitt.edu

Received 23 January 2012, revised 20 August 2012, accepted 19 September 2012

1996). For this reason, DEX has been used in veterinary and clinical settings as an anesthetic adjuvant (Sinclair, 2003; Bekker & Sturaitis, 2005). In neuroimaging studies, DEX can be used as a supplement for reducing minimum alveolar concentration of volatile anesthetics (Segal *et al.*, 1988; Savola *et al.*, 1991), and this combination may also prolong the desired effects of DEX. Thus, DEX + ISO anesthesia is attractive for fMRI studies, but its impact on neuronal activity and hemodynamic responses is not known. In the present study, we investigated the effects of DEX at doses relevant to published fMRI studies on baseline and evoked neurovascular activities by obtaining neuronal, CBF, vessel diameter and fMRI measurements from the rat somatosensory cortex.

Materials and methods

Twenty-five male Sprague–Dawley rats (260–450 g; Charles River Laboratories, Wilmington, MA, USA) were used, following an animal protocol approved by the University of Pittsburgh Institutional Animal Care and Use Committee, in accordance with the National Institutes of Health Guide for the Care and Use of Laboratory Animals. Twenty-one rats were used for non-fMRI studies, and four rats were used for fMRI studies with DEX + ISO anesthesia.

Animal preparation

The rats were initially anesthetised with 5% ISO in O_2-enriched air (30–35% inspired O_2) for intubation. Then, lidocaine gel (2%) was applied locally for placement of catheters in a femoral artery and vein under 2–2.5% ISO. Atropine was not used in the present studies, because its anticholinergic activity can cause adverse cardiovascular effects with DEX administration [for a review, see Sinclair (2003)]. The respiration rate and ventilation volume of the ventilator (TOPO; Kent Scientific, Torrington, CT, USA) were adjusted to maintain normal blood gas levels throughout experiments. Approximately 0.1 mL of blood was withdrawn from the femoral artery for measurement of the arterial partial pressure of oxygen (P_{O_2}), arterial partial pressure of carbon dioxide (P_{CO_2}) and pH with a blood gas analyser (Stat Profile, Nova Medical Corp., Waltham, MA). For non-fMRI physiological studies, the rats were placed in a stereotaxic frame (SR-5R; Narishige, Tokyo, Japan). Lidocaine gel (2%) was applied at pressure points of the stereotaxic frame, and 0.3 mL of 2% lidocaine was administered under the skin over the targeted craniotomy location. A custom-made recording chamber (outer diameter, 2.2 cm) was mounted on the exposed skull over the forepaw cortical area with dental acrylic. A 5 × 7-mm portion of the skull, centered 3.5-mm lateral and 1.5-mm rostral from bregma, was thinned with a dental drill, and then removed with forceps. The cerebrospinal fluid was released by performing a dural puncture of the cisterna magna prior to duratomy, to minimise herniation. The dura mater over the forepaw cortical area was resected. Both the chamber and the dural puncture site were then sealed with agarose gel (typically 0.4%) at body temperature.

The anesthesia and breathing gas mixture were adjusted to 1.3–1.4% ISO in O_2-enriched air (25–30% inspired O_2) for at least 30 min before experiments were started. During experimental recordings, the mean arterial blood pressure (MABP), heart rate, respiration rate, end-tidal CO_2, O_2, N_2O and ISO levels were monitored (Capnomac Ultima; Datex Engstrom, Tewksbury, MA, USA) and recorded with a polygraph data acquisition system (MP150 and ACK100W Acknowledge; Biopac Systems, Goleta, CA, USA). Rectal temperature was maintained at 37.0 °C with a feedback-controlled heating pad (40-90-8C; FHC, Bowdoinham, ME, USA).

Experimental recordings of evoked somatosensory activity were performed under 1.3–1.4% ISO. After these experiments, 50 μg/kg DEX (Dexdomitor; Pfizer, NY, USA) was injected intravenously as a bolus, and the ISO level was reduced to 0.5%. Fifteen minutes after the bolus injection, continuous intravenous infusion of DEX at a rate of 50 μg/kg/h was commenced. The infusion liquid also contained pancuronium bromide (1.5 mg/kg/h) and 5% dextrose. It should be noted that a dose rate of 50 μg/kg/h DEX is equivalent to 100 μg/kg/h MED, which is the typical dose rate used in most published fMRI studies (Ramos-Cabrer *et al.*, 2005; Weber *et al.*, 2006, 2008; Pawela *et al.*, 2008, 2009; Zhao *et al.*, 2008; Airaksinen *et al.*, 2010; Angenstein *et al.*, 2010; Seehafer *et al.*, 2010; Williams *et al.*, 2010; Krautwald & Angenstein, 2012; Nasrallah *et al.*, 2012).

For electrical stimulation, two needle electrodes were inserted between digits 2 and 4 under the palmar skin of either the left or right forepaw. Electrical pulses were generated with a waveform generator (Master 8; AMPI, Israel) and delivered with a constant current isolator (Iso-Flex; AMPI) to the forepaw contralateral to the recording site. Electric pulses with a width of 1 ms and a current of ≤ 1.5 mA were delivered for 10 s. No MABP change resulting from the stimulation was observed.

Experimental designs

Three major experiments were performed: (i) evoked neural activity and hemodynamic responses were recorded under DEX only vs. DEX + ISO vs. DEX + N_2O; (ii) spontaneous neural activity and baseline hemodynamics were recorded under ISO only vs. DEX + ISO; and (iii) evoked neural activity and hemodynamic responses under DEX + ISO were characterised. All functional studies under DEX were performed at least 30 min after the bolus injection of DEX. Neural activities [i.e. local field potentials (LFPs) and multiple unit activity (MUA)] were measured with a metal microelectrode; CBF was measured with laser Doppler flowmetry (LDF); vessel diameters were measured with optical imaging; and blood oxygenation level-dependent (BOLD) fMRI was performed with a 9.4-T magnetic resonance imaging scanner. Specific experiments were as follows (for a summary, see Table 1).

Experiment 1.1 – Evoked LFP and CBF responses under DEX only

To examine whether robust and stable evoked hemodynamic responses can be obtained under DEX-only anesthesia, electrical stimulation at a frequency of 3, 4, 6, 8, 9, 10 or 12 Hz for 10 s with a 70-s interstimulus interval (ISI) was intermittently delivered to the forepaw to evoke LFP and CBF responses in the somatosensory cortex. These experiments were conducted in five rats, and experimental recording lasted for > 120 min, during which DEX alone was continuously infused (50 μg/kg/h). To attempt to extend the effects of DEX demonstrated by Pawela *et al.* (2009), the infusion dose rate was increased from 50 μg/kg/h to 150 μg/kg/h (equivalent to 300 μg/kg/h MED) 120–156 min after the initial DEX bolus administration in three rats, and cortical evoked responses to forepaw stimulation (4, 6, 8, 10 or 12 Hz for 10 s with a 70-s ISI) were recorded. The stimulation frequency over all experiments was randomised between trials. At least two trials were recorded for each frequency in all experiments.

TABLE 1. Summary of experiments

Experiment no.	Content	Number of rats	Stimulation	Results
1.1	Evoked LFP and CBF responses under DEX only	5 for 50 μg/kg/h DEX 3 for 150 μg/kg/h DEX	3, 4, 6, 8, 9, 10 or 12 Hz for 10 s (ISI, 70 s)	Fig. 2
1.2	Comparison between DEX + ISO and DEX + N_2O conditions	7	3, 6, 9 and 12 Hz for 10 s (ISI, 70 s), 2 runs for each frequency	Fig. 3
1.3	Effective duration of DEX + ISO for functional studies	6	8 Hz for 10 s (ISI, 70 s), typically 2 or 5 runs	Fig. 4
2.1	Baseline MUA and LFP measurements before and after DEX administration	9	Not applicable	Fig. 5
2.2	Baseline CBF and vessel diameter measurements before and after DEX administration	15	Not applicable	Fig. 6
3.1	Frequency-dependent evoked LFP and CBF measurements under DEX + ISO	7	4, 6, 8, 10 and 12 Hz for 10 s (ISI, 70 s), 2 runs for each frequency	Fig. 7
3.2	Frequency-dependent BOLD fMRI measurements under DEX + ISO	4	4, 6, 8, 10 and 12 Hz for 10 s (ISI, 70 s), 20–46 runs for each frequency	Fig. 8
3.3	Evoked arterial and venous vessel diameter measurements under DEX + ISO	11	8 Hz for 10 s (ISI, 70 s), 5 runs	Fig. 9

Experiment 1.2 – Comparison between DEX + ISO and DEX + N_2O conditions

To examine the effect of inspired N_2O on evoked responses in DEX-sedated rats, LFP and CBF responses to forepaw stimulation at four different frequencies (3, 6, 9 or 12 Hz for 10 s with a 70-s ISI) were recorded under DEX + N_2O (30% O_2/70% N_2O) and DEX + ISO (< 0.5% ISO in 30% O_2/70% N_2) in seven rats. It should be noted that ISO did not decrease to zero for a long time after the anesthetic vaporiser was completely turned off (> 1 h). As 0.1% ISO has almost no synergistic effect in combination with N_2O (Sloan *et al.*, 2010), experiments under DEX + N_2O were initiated when the ISO level was < 0.1%.

Experiment 1.3 – Effective duration of DEX + ISO for functional studies

To examine the stability of evoked responses over time, LFP and CBF responses to forepaw stimulation (8 Hz for 10 s with a 70-s ISI) were monitored for > 180 min during continuous infusion of DEX (50 μg/kg/h) with ISO (0.1–0.5%) in six rats. Two to five 8-Hz stimulation runs were recorded and averaged. To compare the effects of DEX + ISO and those of ISO only, LFP and CBF responses evoked by 10 s of 8-Hz stimulation (ISI of 70 s) were also recorded under ISO only. Five runs were averaged.

Experiment 2.1 – Baseline MUA and LFP measurements before and after DEX administration

To examine the effects of DEX on spontaneous neural activities, MUA and LFP were recorded for 5 min under ISO only and DEX + ISO in the absence of evoked stimulation in nine rats.

Experiment 2.2 – Baseline CBF and vessel diameter measurements before and after DEX administration

To examine the effects of DEX on baseline CBF and pial vessel diameters, LDF was performed simultaneously with pial vessel imaging under ISO only and DEX + ISO in 15 rats. The baseline CBF level and pial vessel diameters were compared between these two conditions.

Experiment 3.1 – Frequency-dependent evoked LFP and CBF measurements under DEX + ISO

LFP and CBF responses to forepaw stimulation at five different frequencies (4, 6, 8, 10 and 12 Hz for 10 s with a 70-s ISI) were recorded under DEX + ISO in seven rats.

Experiment 3.2 – Frequency-dependent BOLD fMRI measurements under DEX + ISO

BOLD fMRI responses to forepaw stimulation at five different stimulation frequencies (4, 6, 8, 10 and 12 Hz for 10 s with an 80-s ISI) were recorded under DEX + ISO in four rats. A total of 20–46 runs were repeated for each frequency.

Experiment 3.3 – Evoked arterial and venous vessel diameter measurements under DEX + ISO

Pial vessel diameters were measured during 10 s of forepaw stimulation at a frequency of 8 Hz with an ISI of 70 s in 11 rats. Five runs were performed.

Data acquisition

Optical imaging

Prior to the physiological experiments described above, the forepaw area was mapped with flavoprotein autofluorescence imaging over the primary somatosensory cortex under 1.3–1.4% ISO (Vazquez *et al.*, 2010b, 2012). Flavoprotein autofluorescence images were acquired using an imaging software (MetaMorph, Molecular Devices, CA, USA) on an epi-fluorescence microscope (MVX-10; Olympus, Tokyo, Japan) equipped with a ×1 (0.25 NA) objective (Olympus) and a digital cooled-CCD camera (1392 × 1040 imaging pixels, 6.45 × 6.45 μm^2/pixel, CoolSnap HQ2; Photometrics, Princeton, NJ, USA). A mercury lamp light source coupled to a low-noise power supply (100 W; Opti Quip, Highland Mills, NY, USA) was used. The transmitted light was filtered between 450 and 490 nm while the camera recorded the fluorescence emission between 500 and 550 nm. Images were captured at 10 frames/s with a field of view of 5.7 × 4.3–8.9 × 6.7 mm^2, depending on the microscope magnification. The camera's exposure time was set to

100 ms for an effective pixel resolution between 15.4 and 25.6 μm. Forepaw stimulation was performed at the optimal frequency of 12 Hz for 2 s with an ISI of 16 s. Ten runs were repeated and averaged to improve the signal-to-noise ratio.

Images of the cortical surface were captured to measure the diameter of pial vessels (Experiments 2.2 and 3.3). For this purpose, oblique light guides transmitting filtered yellow–green light (570 ± 10 nm) connected to a halogen light source (250 W; Thermo-Oriel, Stratford, CT, USA) were used for illumination. At this wavelength, the light absorption of oxyhemoglobin and that of deoxyhemoglobin are nearly equal, and thus both arteries and veins are equally visible. To prevent artefacts stemming from the LDF probe (780-nm laser light), a low-pass interference filter (< 700 nm) was placed in front of the camera. Images were captured over a field of view of 1.7 × 1.2–8.9 × 6.6 mm^2 with an effective pixel resolution between 2.56 and 6.40 μm for the baseline study (Experiment 2.2), and over a field of view of 1.9 × 1.6–3.3 × 2.5 mm^2 at 10 frames/s with an effective pixel resolution between 2.6 and 5.1 μm for the functional study (Experiment 3.3).

MUA, LFP and CBF measurements (all experiments except for 3.2)

On the basis on the functional map generated, a microelectrode with a tip diameter of 5 μm (Carbostar-1; Kation Scientific, Minneapolis, MN, USA) was placed at a depth of ~0.3 mm below the cortical surface of the forepaw area (Fig. 1) to record neural activity extracellularly. Neural activity was recorded with an electrophysiological data acquisition system (MAP; Plexon, Dallas, TX, USA) at a 1-kHz sampling rate. Baseline neural activity (Experiment 2.1) was acquired for a 5-min period. MUA data were bandpass filtered between 400 Hz and 1 kHz, and LFP activity was bandpass filtered between 3.3 and 88 Hz.

A needle-type LDF probe with tip diameter of 450 μm (PeriFlux 4001 Master System; Perimed, Sweden) was placed on the cortical surface over the forepaw area, avoiding large pial vessels, to measure parenchymal CBF (Fig. 1). Relative changes in CBF were acquired by the LDF system with a time constant of 0.03 s, and recorded with the polygraph data acquisition software at a frequency of 100 Hz.

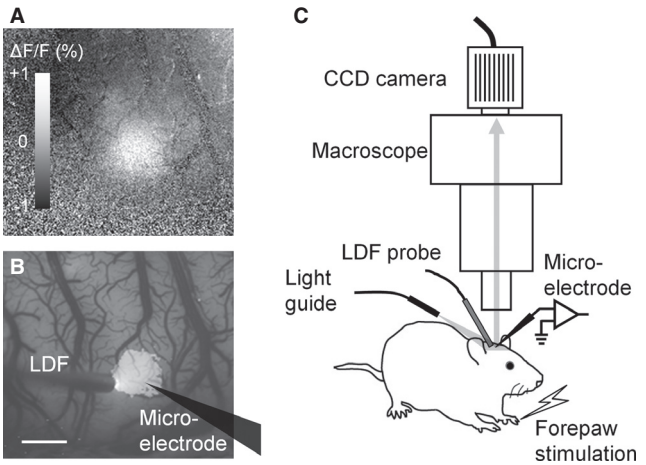

FIG. 1. Optical imaging of flavoprotein autofluorescence signal and recording setup schematic. (A) The cortical forepaw area mapped with flavoprotein autofluorescence in an ISO-anesthetised rat is shown. The white region indicates an increase in autofluorescence evoked by electrical forepaw stimulation. The map was averaged over 0–1 s after stimulation onset. The gray scale bar indicates the change in autofluorescence (ΔF) from the pre-stimulation baseline (F). (B) Pixels with an intensity of > 67% of the peak intensity (defined as belonging to the hot spot) in the activity map (A) are overlaid on the baseline autofluorescence image. An LDF probe and a microelectrode were placed within or in the vicinity of the hot spot for recording CBF and LFP, respectively. The microelectrode location is drawn on the map. Scale bar: 1 mm. (C) Schematic of the recording setup for the forepaw rat model. An LDF probe, microelectrode and light guide were arranged under the microscope. The cortical surface was illuminated with yellow–green light (570 ± 10 nm), and video images were captured every 100 ms with a CCD camera mounted on the microscope.

BOLD fMRI (Experiment 3.2)

BOLD fMRI experiments were performed on a 9.4-T MRI system with a Unity INOVA console (Varian, Palo Alto, CA, USA). The gradient coil used is actively shielded, and has an inner diameter of 12 cm, a maximum gradient strength of 40 G/cm, and a rise time of 0.12 ms (Magnex, Abington, UK). A surface coil (diameter, 2.3 cm) was positioned on top of the rat's head for imaging. The magnetic field homogeneity was optimised by localised shimming to yield a typical water spectrum line-width of ~20 Hz. All fMRI images were acquired with a gradient echo echo-planar imaging sequence with an echo time of 20 ms, a repetition time of 1000 ms, an in-plane matrix of 64 × 64, a field of view of 2.3 × 2.0 cm, and a slice thickness of 2 mm, over four contiguous slices. All data were collected within 2 h after the bolus DEX administration.

Data analysis

All of the data were analysed with MATLAB (Mathworks, Natick, MA, USA). Optical images, LFPs, CBF data and BOLD fMRI data were averaged over multiple runs from identical stimulus frequency conditions. Analyses were performed on each rat separately before group averaging. All graphs, including scatter plots, box plots, and power law curve fitting, were produced with ORIGIN 7 (OriginLab Corp., MA, USA).

Flavoprotein autofluorescence imaging map

To determine forepaw area, activation maps were generated from flavoprotein autofluorescence images by calculating the relative increase in fluorescence ($\Delta F/F$). The differential image (ΔF) was obtained by subtracting the average image over 1 s prior to stimulation (F) from the average image over the initial 1 s of stimulation. The maps were smoothed by use of a Gaussian kernel with a width of 5 × 5 pixels, and pixels over a threshold of > 67% of the largest increase in fluorescence ($\Delta F/F$) were considered to be part of the active area (Fig. 1).

Vessel diameter measurement (Experiments 2.2 and 3.3)

Pial arteries and veins were visually distinguished on the basis of the differences in their color under the microscope with white light illumination (arteries are light red, and veins are dark red). The intraluminal vessel diameter was calculated from 570-nm optical images by placing a region of interest (ROI) with a four-pixel width perpendicular to the vessel direction. The image within the ROI was linearly interpolated, and the intensity along the four-pixel direction was then summed to obtain projected intensity profiles. This yielded the intraluminal vessel profile, and its full-width-at-half-minimum was measured. Assuming that the vessel is cylindrical, the actual diameter corresponds to 15.5% over the full-width-at-half-minimum value (Vazquez *et al.*, 2010a).

For the study of evoked vessel diameter changes, feeding arteries and draining veins of the active area were chosen. To evaluate whether vessel diameter changed during stimulation, vessel diameters sampled from 5 s prior to stimulation and the 10-s stimulation period were compared by use of a Kruskal–Wallis test (one-way analysis of variance by ranks). If a significant difference was found in the median ($P < 0.05$), the vessel diameter was considered to significantly change with stimulation. To calculate evoked vessel diameter changes as a function of time (Experiment 3.3), the vessel diameters were normalised by their baseline value (5 s prior to stimulation onset). The maximal diameter change during the 10-s stimulation period was then extracted after low-pass filtering the time course with a cut-off frequency of 2 Hz. To examine the dynamic properties of the changes in vessel diameter, normalised time courses were averaged across all active arteries and veins.

LFP, MUA and CBF data

The evoked LFP data were first fully rectified and summed over the 10-s stimulation period. The summed LFP data were then multiplied by the sampling (0.001 s). For the baseline neural activity data (Experiment 2.1), the mean spike firing rate and LFP power spectral bands were determined for the 5-min recording in each rat. MUA and LFP signals were separated by bandpass filtering between 400 Hz and 1 kHz and between 3.3 and 88 Hz, respectively. To determine the mean spike firing rate (spikes/s), a one standard deviation (SD) threshold was applied for the ISO-only and DEX + ISO conditions (the SDs from both anesthesia conditions were averaged). A spike was considered to be present for each 1-ms time point where the MUA intensity exceeded the SD threshold (i.e. 1 spike/ms). The spike firing rate was obtained for each 1-s time bin, and the mean spike firing rate for 5 min was calculated. To determine the LFP power over specified spectral bands, the 5-min LFP data were Fourier-transformed. Then, the spectrum was divided into delta (1 to < 4 Hz), theta (4 to < 8 Hz), alpha (8 to < 13 Hz), beta (13 to < 30 Hz), and gamma (30 to < 50 Hz).

The CBF data were low-pass filtered with a 5-Hz cut-off frequency. The filtered CBF data were then normalised by their baseline value (5-s period prior to stimulation onset). The normalised CBF responses were summed over the 10-s stimulation period, and multiplied by the sample rate of 0.01 s. To examine the dynamic properties of the changes in CBF, each time course was normalised by its peak intensity and averaged across all rats.

BOLD fMRI

Correlation coefficients between the voxel-wise time courses and a canonical reference function were calculated. The fMRI data recorded for 8-Hz stimulation were used to determine the ROI for analyzing frequency-dependent studies. The ROI was defined as the 20 voxels with the highest correlation coefficients in the forepaw cortical area. Then, time courses were obtained from the ROI, and percentage signal changes were calculated from the baseline, the average value over the 5-s period prior to stimulation onset. A positive BOLD response was integrated over the 10-s stimulation period, and a post-stimulus undershoot was integrated over 5–25 s after stimulation offset. In each rat, the integral BOLD responses were determined for the five stimulation frequencies, and these were normalised by their maximum to reduce inter-animal variation.

Statistical analysis

Non-parametric statistical tests were used to compare medians. *P*-values of < 0.05 were considered to be statistically significant. All data are expressed as median and interquartile range (IQR), unless otherwise specified.

Results

Blood gas measures of all experiments and their statistical results (Mann–Whitney *U*-test, Bonferroni-corrected) are reported in Table 2. For non-fMRI experiments, DEX administration significantly reduced P_{O_2} ($P = 0.0002$,) and S_{O_2} ($P = 0.0054$), and increased hematocrit ($P = 0.0048$) and the hemoglobin ($P = 0.0051$) concentration, although they remained within normal physiological ranges (see ISO only vs. DEX50 + ISO for non-fMRI in Table 2). No significant difference was found in blood gas measurements between DEX + ISO and DEX-only conditions. For fMRI experiments, no significant difference was found in blood gas measurements between ISO-only and DEX + ISO conditions. However, P_{CO_2} was significantly lower in non-fMRI experiments [$P = 0.0046$; see DEX + ISO (non-fMRI) vs. DEX + ISO (fMRI) in Table 2], possibly owing to hypocapnic conditions in fMRI rats.

TABLE 2. Blood gas tests

Blood gas parameters	Non-fMRI				fMRI	
	ISO only ($N = 21$)	DEX50 + ISO ($N = 16$)	DEX50 only ($N = 5$)	DEX150 only ($N = 2$)†	ISO only ($N = 4$)	DEX50 + ISO ($N = 4$)
Temperature (°C)	37.4 (0.2)	37.3 (0.3)	37.4 (0.1)	37.3 (0.1)	37.0 (0.2)	37.2 (0.3)
pH	7.511 (0.049)	7.482 (0.049)	7.487 (0.054)	7.470 (0.009)	7.495 (0.037)	7.470 (0.008)
P_{CO_2} (mmHg)	36.1 (5.6)	38.2 (4.7)	38.4 (1.6)	37.1 (0.5)	31.8 (4.9)***	30.7 (7.1)***
P_{O_2} (mmHg)	125.1 (16.0)	108.2 (8.0)*	102.8 (19.1)	108.6 (9.3)	144.3 (15.2)**	118.6 (22.5)
S_{O_2} (%)	98.6 (1.2)	97.7 (0.9)****	98.3 (1.6)	98.4 (0.3)	98.4 (0.8)‡	98.2 (0.0)§
Hct (%)	37.0 (2.3)	40.0 (4.0)****	38.0 (4.0)	42.0 (2.0)	32.0 (6.0)‡	34.0 (0.0)§
Hb (g/dL)	12.4 (0.6)	13.2 (1.3)****	12.5 (1.2)	13.9 (0.6)	12.4 (0.6)‡	11.5 (0.0)§

DEX50, DEX 50 μg/kg/h, intravenous; DEX150, DEX150 μg/kg/h, intravenous; Hb, hemoglobin; Hct, hematocrit; ISO, 1.3–1.4% for ISO only, 0.1–0.5% with DEX; *N*, numbers of rats used. All values are presented as medians (IQRs). Multiple comparisons were performed for four conditions from non-fMRI experiments. Similarly, multiple comparisons were performed for four conditions from both non-fMRI and fMRI experiments (ISO only and DEX50 + ISO). Thus, the significant *P*-value of 0.05 is actually 0.0083 after Bonferroni correction. *$P < 0.05$ vs. ISO only in non-fMRI group by Mann–Whitney *U*-test with Bonferroni correction. **$P < 0.05$ vs. DEX + ISO in non-fMRI group by Mann–Whitney *U*-test with Bonferroni correction. ***$P < 0.05$ vs. DEX + ISO in non-fMRI group by Mann–Whitney *U*-test with Bonferroni correction. ****$P < 0.05$ vs. ISO only in non-fMRI group by Mann–Whitney *U*-test with Bonferroni correction. †Blood gas measures available for only two of three rats used in this condition. ‡$n = 3$. §$n = 1$.

DEX and ISO combination for functional studies

DEX only (Experiment 1.1)

In almost all MED-sedated rat fMRI studies, recording was performed under MED only (typically 100 μg/kg/h, equivalent to 50 μg/kg/h DEX). Therefore, somatosensory evoked LFP and CBF responses from forepaw cortical area in five rats were first recorded under intravenous DEX only (50 μg/kg/h) (Fig. 2A, left column). Although robust, stimulation frequency-dependent CBF responses were observed, consistent with earlier fMRI studies (Zhao *et al.*, 2008; Pawela *et al.*, 2009), periods of epileptic neural discharges followed by electrical silence were also observed, resulting in abnormally prolonged CBF responses (see open arrowheads above the LFP and CBF traces in Fig. 2A, left column). Epileptic responses to 10 s of stimulation were observed in runs at 119–177 min after the initial DEX administration in four of the five rats tested (note – the DEX dose rate was modified for the remaining rat prior to the time period where epileptic activity was observed; Fig. 2B). These results suggest that evoked responses are prone to become epileptic when DEX is infused at a rate of 50 μg/kg/h for longer than 120 min.

To attempt to avoid this epileptic effect, the DEX dose was increased from 50 to 150 μg/kg/h after 120 min from the initial dose in three rats (see two rats' data in Fig. 2). However, epileptic LFP and CBF responses were elicited as soon as stimulation studies were started (Fig. 2A, right column; Fig. 2B) in all three rats tested. Changes in MABP did not correlate with, or precede, the initiation of the epileptic discharges, suggesting that a systemic physiological perturbation did not trigger the epileptic-like incident at these dose rates (compare MABP and LFP traces in Fig. 2A and B). However, supplementing the intravenous DEX administration at 50 μg/kg/h with inspired ISO at 0.1–0.5% successfully mitigated the stimulation-evoked epileptic response in 15 of 16 rats over a median recording time of 188 min (IQR, 79.3 min; minimum, 123 min; maximum, 306 min). Only one rat showed epileptic responses 171 min after the initial DEX administration under DEX + ISO at 0.5%. Therefore, the rest of the experiments were performed under intravenous DEX at 50 μg/kg/h and ISO (0.1–0.5%, typically ~0.3%) to avoid the possible development of epileptic responses.

DEX with N_2O (Experiment 1.2)

Inhaled N_2O is widely used with other anesthetics to enhance analgesic effects in clinical, veterinary and research settings. However, N_2O is an *N*-methyl-D-aspartate receptor antagonist (Jevtovic-Todorovic *et al.*, 1998; Mennerick *et al.*, 1998) that is known to reduce hemodynamic responses (Norup Nielsen & Lauritzen, 2001; Gsell *et al.*, 2006). Indeed, inhaled N_2O suppresses somatosensory evoked hemodynamic responses in combination with ISO at ~1.4% in rats (Masamoto *et al.*, 2007; Kim *et al.*, 2010). Thus, the effect of supplementary inhaled N_2O on LFP and CBF responses was also tested in seven DEX-sedated rats (Fig. 3). As a control, evoked LFP and CBF responses were first recorded under DEX + ISO in O_2-enriched air (30%O_2 and 70%N_2). ISO was then discontinued, and the inspired air was replaced with a mixture of 30%O_2 and 70%N_2O. No significant changes in vascular physiological parameters were found (Table 3). Additionally, N_2O inhalation did not change the baseline CBF (see control vs. test panels in Fig. 3A, and left panel in Fig. 3B). However, the evoked LFP responses at 6 and 9 Hz under N_2O were significantly smaller than those in the control condition ($P = 0.0262$ for 6 Hz, $P = 0.0478$ for 9 Hz, $n = 7$ rats, Mann–Whitney *U*-test). Similarly, the evoked CBF responses at 6, 9 and 12 Hz under N_2O were significantly smaller than those under the control condition ($P = 0.0111$ for 6 Hz, $P = 0.0006$ for 9 Hz, $P = 0.0379$ for 12 Hz, $n = 7$ rats, Mann–Whitney *U*-test).

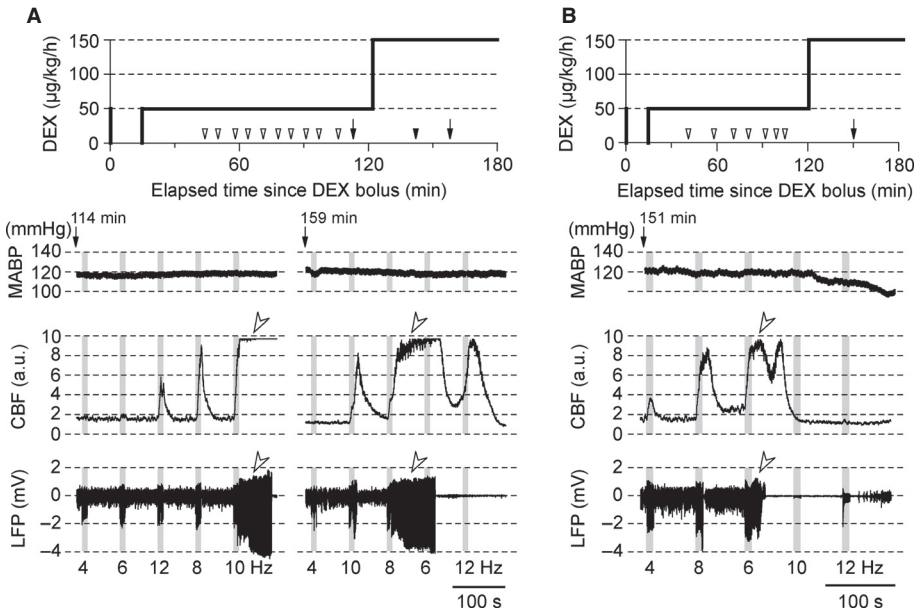

FIG. 2. CBF and LFP responses in DEX-sedated rats without supplemental ISO. (A, B) Examples obtained from two rats. Evoked responses are prone to induce epileptic activity after ~120 min from the initial DEX administration. First row – intravenous infusion of DEX plotted as a function of time from the initial bolus injection of 50 μg/kg (0 min). Open arrowheads on the time scale indicate the beginning of a block of five stimulation runs (each consisting of 10 s of forepaw stimulation with a 70-s ISI). Arrows with filled arrowheads indicate a block containing epileptic responses. Traces of MABP (second row), CBF (third row) and LFP (fourth row) responses from the blocks indicated by the arrows in the first row are shown. The time elapsed from the DEX bolus injection is shown above the MABP trace. Gray vertical bars in each panel indicate 10-s stimulation periods, and the numbers under the LFP traces indicate the stimulation frequencies, which were delivered in a pseudo-randomised order. Open arrowheads in the CBF and LFP traces point to apparent epileptic responses without any change in MABP.

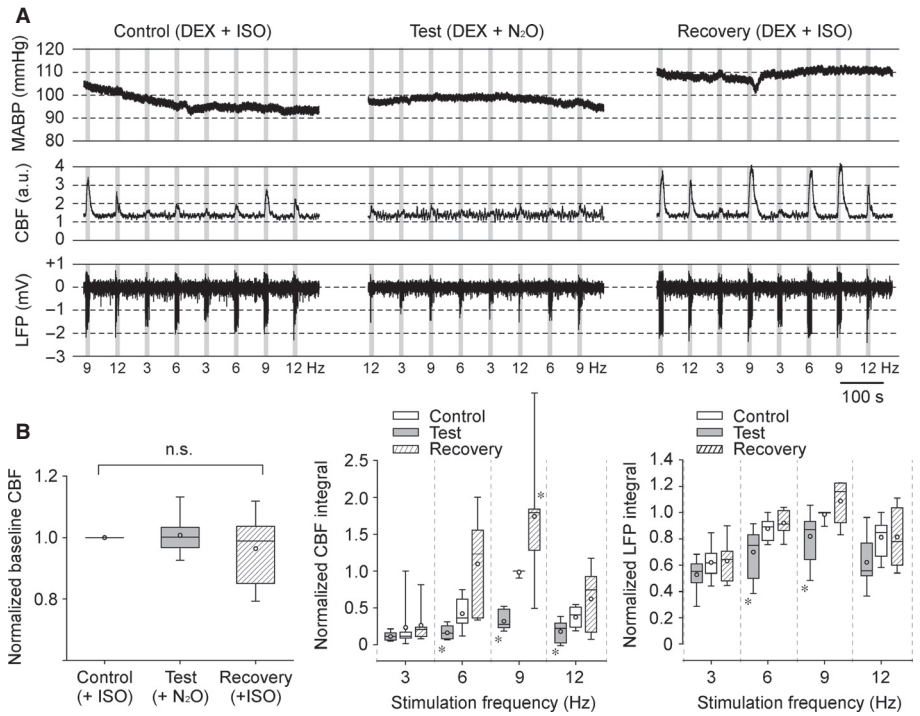

FIG. 3. N_2O suppresses evoked CBF responses in DEX-sedated rats. (A) An example from one representative rat among seven rats tested. MABP (first row), CBF (second row) and LFP (third row) responses to stimulation at four different frequencies during control (left column), test (middle column) and recovery (right column) conditions are shown. Recording under the control condition started 104 min after the bolus DEX administration (ISO, 0.27%; O_2, 29.1%; N_2O, 0.0%); the test condition started at 130 min (ISO, 0.07%; O_2, 28.9%; N_2O, 69.3%); and the recovery condition started at 150 min (ISO, 0.24%; O_2, 29.8%; N_2O, 4.06%). Each condition consists of two 4-stimulation frequency runs. Gray vertical bars – 10-s stimulation. Numbers under LFP traces – stimulation frequency. (B) Summary plots from seven rats (see also Table 3). Box plots for the baseline CBF level (left panel), CBF response amplitude (middle panel) and LFP responses (right panel) for four stimulation frequencies during control (open box), test (gray box) and recovery (shadowed box) conditions are shown. The CBF baseline was normalised to the control condition in each rat. No significant difference (n.s.) was found in the median of the baseline CBF level between control, test and recovery conditions [Kruskal–Wallis test, $\chi^2(2, N = 21) = 1.3015$, $P = 0.5217$]. For CBF and LFP responses, the integrals of LFP and CBF responses over the 10-s stimulation period were calculated for each stimulation frequency, and normalised to their maximum in each rat. A significant difference was found in the medians of CBF responses between control, test and recovery conditions [Friedman test, $\chi^2(2, N = 7) = 33.86$, $P = 0.0000000443533$]. Similarly, a significant difference was found in the medians of LFP responses [Friedman test, $\chi^2(2, N = 7) = 19.61$, $P = 0.0000553021$]. A *post hoc* analysis (Mann–Whitney *U*-test) revealed that CBF responses at 6, 9 and 12 Hz and the LFP responses at 9 and 12 Hz in the test condition were significantly smaller than those in the control condition (*$P < 0.05$). Furthermore, the CBF response at 9 Hz in the recovery condition was significantly larger than in the control condition (*$P < 0.05$).

Upon replacement of the O_2/N_2O breathing mixture with ISO and O_2-enriched air, both LFP and CBF responses fully recovered (see recovery, right panel in Fig. 3A and B), although the CBF response at 9 Hz in the recovery condition was significantly larger than that under control conditions ($P = 0.0221$, $n = 7$ rats, Mann–Whitney *U*-test).

Overall, N_2O significantly suppressed CBF responses to a larger extent than LFP responses (middle vs. right panel in Fig. 3B). For instance, the CBF response to 9-Hz stimulation under DEX + N_2O was only 28% (median) of the response under DEX + ISO, whereas the LFP response was 87% of the control. These results suggest that supplementary ISO (< 0.5%) is a more suitable combination with DEX than N_2O.

DEX with ISO (Experiment 1.3)

The use of supplementary ISO, a known vasodilator, did not seem to affect the baseline CBF level under DEX anesthesia (compare Figs 2 and 3). Similarly, at a level of 0.5%, ISO did not appear to decrease the amplitude of the evoked LFP response; however, the amplitude of the CBF response was slightly smaller that that obtained under DEX-only sedation (compare Figs 2 and 3), although it was still robust. As compared with ISO only, DEX + ISO significantly increased evoked response amplitudes. At a median time of 91.0 min (IQR, 16.0 min) after the initial DEX administration, the LFP and CBF responses to 10 s of 8-Hz forepaw stimulation under DEX + ISO were 1.5-fold and 3.7-fold larger, respectively, than those under ISO only (both LFP and CBF responses became significantly larger; $P = 0.0313$, $n = 6$ rats, Wilcoxon signed rank test). No significant difference in MABP was found between these two conditions ($P = 0.1563$, $n = 6$ rats, Wilcoxon signed rank test). Our data indicate that DEX + ISO significantly enhances evoked hemodynamic responses.

However, this robust CBF response under DEX + ISO anesthesia was not sustainable over a long experimental time window, despite preserved LFP responses (Fig. 4). In general, the CBF response was robust over the initial 120–180 min. The baseline CBF level tended to decrease over time, becoming unstable. In addition, MABP tended to decrease over time, although it remained within a normal physiological range (80–120 mmHg). Thus, it was necessary to decrease the supplementary ISO level during the course of experimental recording to maintain MABP and obtain robust evoked CBF responses. When the supplementary ISO level was decreased below 0.1%, evoked responses occasionally became epileptic, and thus the ISO level was always maintained above 0.1% (typically, ~0.3%).

TABLE 3. MABP and inspired gas concentrations in experiment 1.2

	Control (DEX + ISO)	Test (DEX + N_2O)	Recovery (DEX + ISO)
Recording onset time from initial DEX administration (min)	96.0 (10.8)	120.0 (8.3)	141.0 (9.8)
MABP (mmHg)	96.5 (3.3)	98.2 (4.8)	113.8 (11.2)
ISO (%)	0.3 (0.1)	0.07 (0.03)	0.2 (0.1)
O_2 (%)	30.8 (2.3)	30.3 (2.4)	30.3 (1.9)
N_2O (%)	0.04 (0.00)	67.1 (2.1)	3.7 (1.8)

Values are medians (IQRs) from seven rats. No significant difference was found in MABP medians between control, test and recovery conditions [Kruskal–Wallis test, $\chi^2(2, N = 21) = 4.9647$, $P = 0.0835$]. Similarly, no significant difference was found in inspired O_2 medians between control, test and recovery conditions [Kruskal–Wallis test, $\chi^2(2, N = 21) = 0.2301$, $P = 0.8913$].

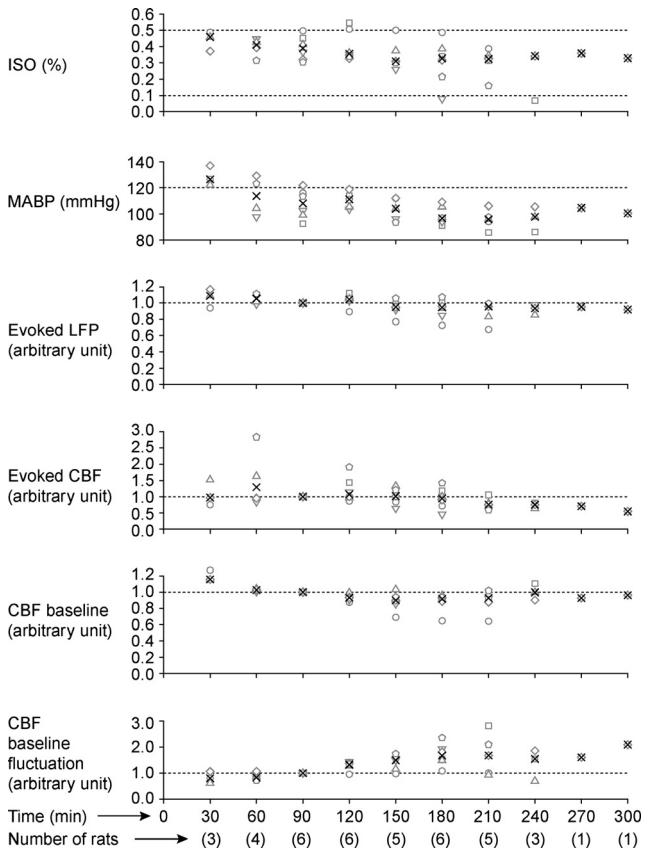

FIG. 4. Effects of DEX on evoked LFP and CBF responses to 8-Hz forepaw stimulation for an extended recording time. ISO, MABP, evoked LFP, evoked CBF, CBF baseline and CBF baseline levels are plotted as a function of time. The integral of the evoked CBF and LFP responses for the 10-s stimulation period are shown. Both the SD and the mean of the CBF baseline for the 5-s pre-stimulation period were obtained, and CBF baseline fluctuation was calculated as SD/mean. The evoked LFP, evoked CBF, CBF baseline and CBF baseline fluctuation were normalised by those at 90 min. At each 30-min time point, data were averaged within ± 15 min of the specific time indicated. Different symbols represent different rats, and black cross marks indicate medians.

Effects of DEX + ISO anesthesia on baseline physiology

Different anesthetics modulate spontaneous neuronal activity and baseline CBF differently (Masamoto *et al.*, 2007). Even with the same anesthetics, the baseline activity is modulated dose-dependently, and affects evoked responses (Masamoto *et al.*, 2009). Therefore, the effect of DEX on baseline neuronal activity and CBF was examined. Bolus administration of intravenous DEX (50 μg/kg) induced bradycardia and a transient increase in MABP followed by a gradual decrease in MABP over time by affecting the peripheral nervous system, consistent with earlier reports (Scheinin *et al.*, 1989; Vickery & Maze, 1989; Bari *et al.*, 1993).

Spontaneous neuronal activity (Experiment 2.1)

Under DEX + ISO anesthesia, MUA was more phasic and the LFP waveforms were broadened (Fig. 5A), suggesting more synchronous neuronal activity. The mean spike firing rate was significantly increased from 3.5 to 6.9 spikes/s (Fig. 5B) by DEX administration ($P = 0.00049362$, $n = 9$ rats, Mann–Whitney *U*-test). To quantify the effect of ISO-only and DEX + ISO conditions on LFP activity, LFP power spectrum bands were compared (Fig. 5C). DEX increased delta band power significantly ($P = 0.0040$, $n = 9$ rats, Mann–Whitney *U*-test), whereas it significantly decreased beta and gamma band power ($P = 0.0040$ for beta, and $P = 0.0005$ for gamma, Mann–Whitney *U*-test).

Baseline vessel diameter (Experiment 2.2)

To examine whether basal CBV is changed by DEX, pial vessel diameters were measured before and after DEX administration (Fig. 6). DEX constricted both arteries and veins (Fig. 6A). The constriction reached a plateau 30 min after the initial bolus administration (Fig. 6B). This observation was consistent in 15 of the 16 rats studied. The medians of arterial and venous diameters at 67.5 min (IQR, 7 min) after initial DEX administration were 77% ($n = 94$) and 74% ($n = 331$), respectively, of those under ISO only (Fig. 6C). No significant difference was found between arterial and venous diameter changes ($P = 0.7546$, Mann–Whitney *U*-test), suggesting that systemic DEX administration equally constricts pial arteries and veins. The degree of constriction was related to the vessel diameter, so that vessels of larger diameter constricted by greater amounts (Spearman's rank correlation, $r_{94} = -0.4031$, $P = 0.000064899$ for artery; $r_{331} = -0.1487$, $P = 0.0067$ for vein).

Baseline CBF (Experiment 2.2)

Systemic administration of DEX significantly decreased baseline CBF in all 15 rats studied, as shown in Fig. 6D ($P = 0.00022289$, $n = 15$ rats, Wilcoxon rank sum test). The median CBF baseline in the DEX + ISO condition was 47% of that in the ISO-only condition, suggesting that intracortical vessels may also constrict.

Characterisation of neuronal and vascular responses under DEX + ISO anesthesia

The optimal stimulation frequency varies with the anesthetic used (Masamoto *et al.*, 2007). Zhao *et al.* (2008) examined the dependence of the hemodynamic response amplitude on forepaw stimulation frequency in rats anesthetised with MED only, and found that the largest BOLD fMRI response was observed at 9 Hz, although no significant difference was found when the response was compared with those at 6–15 Hz. Here, we examined the impact of supplemental ISO administration on neurovascular responses as a function of forepaw stimulation frequency by measuring LFP and CBF and performing BOLD fMRI.

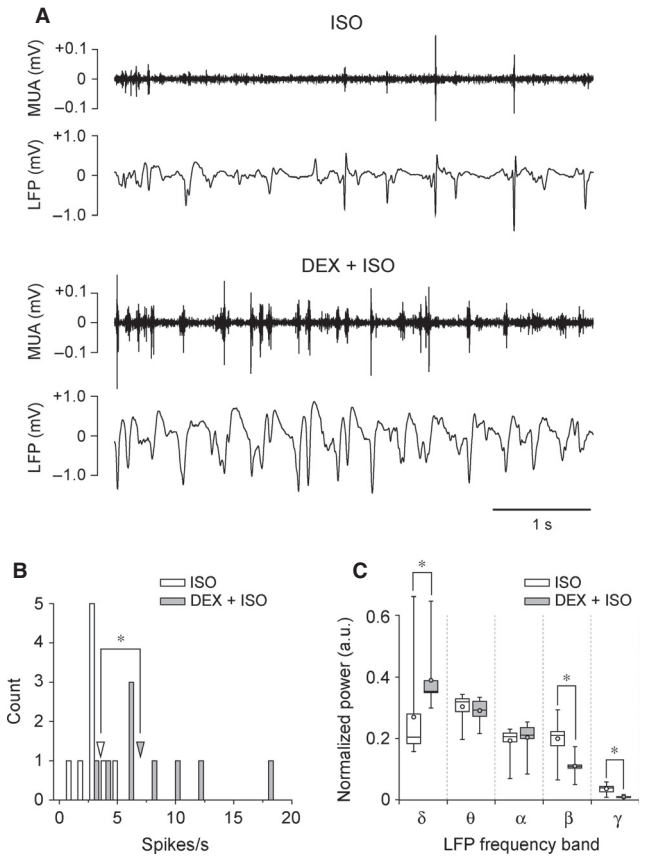

FIG. 5. Intravenous DEX administration makes MUA phasic and broadens the LFP waveform. (A) Spontaneous MUA and LFP recorded for 5 min in one rat are compared with those recorded before (upper two traces) and 33 min after (lower two traces) DEX administration. A 5-s segment is shown for better visualisation. (B) Histogram of spontaneous spike firing rates (open bar, ISO; gray bar, DEX + ISO) with a bin size of 1 s. Open and gray arrowheads indicate the medians of spontaneous spike firing rates for ISO (3.5 spike/s) and DEX + ISO (6.9 spike/s) conditions, respectively. These medians are significantly different (*$P < 0.05$). (C) Comparisons of the LFP power bands before and after DEX administration. Results are shown as box plots (open box, ISO; gray box, DEX + ISO). DEX significantly increased the power of the delta band, whereas it significantly decreased the power of the beta and gamma bands (*$P < 0.05$). In B and C ($n = 9$ rats), recording was started at a median time of 31.0 min (IQR, 4.3 min) after initial DEX administration. Before and after DEX administration, the median ISO levels were 1.3% (IQR, 0.1%) and 0.4% (IQR, 0.1%), respectively; MABP was 84.0 mmHg (IQR, 18.7 mmHg) and 116.1 mmHg (IQR, 23.6 mmHg), respectively.

LFP and CBF (Experiment 3.1)

To determine the stimulation frequency tuning for LFP and CBF responses, their evoked responses at five different stimulation frequencies were measured from seven rats (Fig. 7A). The responses obtained were normalised by the maximum value within each rat to reduce inter-animal variation (Fig. 7B and C). Both LFP and CBF responses differed significantly as a function of stimulation frequency [Kruskal–Wallis test, $\chi^2(4, N = 35) = 26.7897$, $P = 0.000021923$ for LFP; $\chi^2(4, N = 35) = 26.3893$, $P = 0.0000026410$ for CBF]. A *post hoc* analysis (Mann–Whitney *U*-test, Bonferroni-corrected, for a significance level of $P = 0.005$) revealed that LFP responses at 8 Hz were not significantly different from those at 10 Hz ($P = 0.0087$), but were significantly larger ($P = 0.0006$) than responses at the other frequencies (Fig. 7B). Similarly, the CBF response at 8 Hz was significantly larger ($P = 0.0006$, Mann–Whitney *U*-test, Bonferroni-corrected) than responses at all other frequencies (Fig. 7B).

Although the LFP and CBF responses had the same optimal frequency (i.e. 8–10 Hz), their tuning curves differed significantly [Friedman test, two-way analysis of variance by ranks, $\chi^2(1, N = 7) = 21.5753$, $P = 0.00000034020$], indicating a non-linear relationship between LFP and CBF responses. The relationship observed between the LFP and CBF responses (Fig. 7C) was well described by a power law function ($CBF = a LFP^b$, where $a = 1.03 \pm 0.09$ and $b = 3.84 \pm 0.70$, $R^2 = 0.94$). Under DEX-only conditions, CBF was well described by $aLFP^b$, where $a = 1.00 \pm 0.10$ and $b = 3.23 \pm 0.86$ ($R^2 = 0.90$) (data not shown), suggesting no change in neurovascular coupling resulting from supplemental administration of ISO.

Stimulation frequency-dependent BOLD fMRI (Experiment 3.2)

BOLD responses evoked by forepaw stimulation were measured from the somatosensory forepaw cortical area in four DEX + ISO-anesthetised rats for > 3 h. After approximately 2–3 h from the initial DEX administration, baseline signal oscillations became apparent, and the evoked responses became unclear in two rats (not shown). Thus, frequency-dependent BOLD data were averaged over the initial 2 h after DEX bolus injection. Forepaw stimulation induced significant BOLD responses in the contralateral cortical somatosensory area for all frequencies (Fig. 8A). Time courses of frequency-dependent BOLD responses from all four rats are shown in Fig. 8B. In all four rats, similar frequency-dependent trends were observed. The commonly observed post-stimulus undershoot was present regardless of stimulation frequency in all four rats. To obtain stimulation frequency tuning, normalised BOLD signals over the 10-s stimulation period average and over the 20-s post-stimulus offset period average were plotted as a function of stimulation frequency (Fig. 8C). On average, the tunings from both the positive response and the post-stimulus undershoot appeared to be similar; the maximum response was observed at ~10 Hz. The optimal frequency found in BOLD fMRI studies was consistent with the LDF-based CBF results in this study as well as with an earlier MED-only BOLD fMRI report (Zhao *et al.*, 2008).

Evoked pial vessel diameter changes (Experiment 3.3)

Arterial vessel dilation is a major component of the vascular response, whereas venous vessel dilation is minimal during 10 s of forepaw stimulation under either ISO or α-chloralose anesthesia (Hillman *et al.*, 2007; Kim *et al.*, 2007; Vazquez *et al.*, 2010a; Zong *et al.*, 2012). To examine whether this is the case for DEX + ISO anesthesia, the diameter changes in pial arterial and venous vessels were measured (Fig. 9). As seen in a representative example (Fig. 9A), vessel diameter increased not only in pial arteries but also in veins during forepaw stimulation. The diameter changes of arterial vessels were larger than those of venous vessels. The maximal diameter changes in feeding arteries and draining veins of the active area from all 11 rats are shown in Fig. 9B; significant dilation of vessels was found in all arteries [$n = 38$; 3 (2.0) vessels/rat (median and IQR)] during stimulation, and significant diameter changes were found in 85% of veins measured [$n = 80/94$; 7 (3.3) vessels/rat]. Median increases in arterial and venous vessel diameters were 32.2% and 5.8%, respectively (Fig. 9B histogram), which were significantly larger than 0 [$P = 0.000000077397$ for artery ($n = 38$), $P = 0.00000000069148$ for vein ($n = 94$), Wilcoxon signed rank test]. The change in arterial diameter appeared to be greater in smaller arteries, even though this finding was not statistically significant (Spearman's rank correlation coefficient, $r_{38} = -0.2726$,

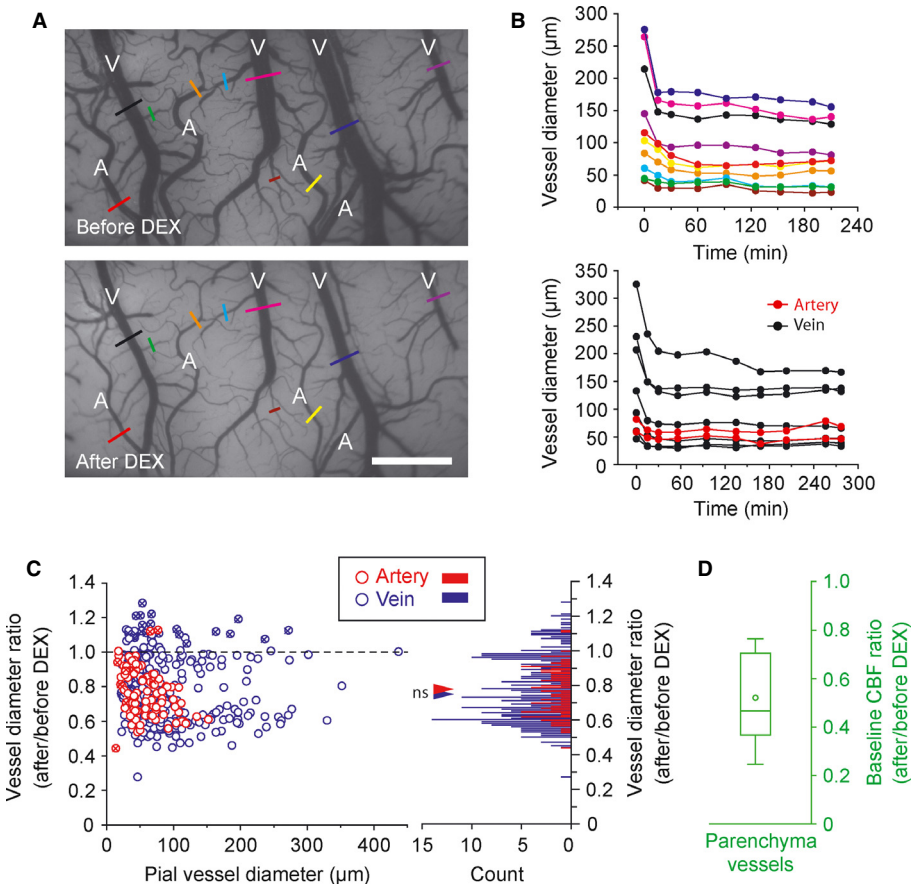

FIG. 6. Intravenous DEX administration equally constricts pial arteries and veins, and decreases baseline CBF. (A) Pial vessel images before and 60 min after bolus DEX administration from one ISO-anesthetised rat are shown. 'A' and 'V' in the image represent arteries and veins, respectively. Quantitative vessel diameters were obtained from the sections indicated by color bars and plotted in the upper panel of (B). Scale bar: 1 mm. (B) Changes in arterial and venous vessel diameters as a function of time from two rats are shown. Time 0 represents the onset of DEX bolus injection. Upper panel – results from the rat shown in (A). MABP was gradually decreased from 126.6 to 92.6 mmHg over time, and ISO level was reduced from 0.51% to 0.32% over time. Lower panel – results from another rat. Red and black represent arteries and veins, respectively. MABP was gradually decreased from 114.0 to 81.8 mmHg over time, and ISO level was reduced from 0.55% to 0.08% over time. (C) Ratios of vessel diameters with and without DEX (94 arteries and 331 veins in 15 rats) – 1.0, no diameter change; < 1.0, vasoconstriction; > 1.0, vasodilation. The effect of DEX on vessel diameter was measured at 67.5 min (IQR, 7 min) after DEX administration. Left panel – relationship between vessel diameter changes induced by DEX administration and basal vessel diameters. Red and blue circles indicate arteries and veins, respectively. The horizontal broken line indicates no diameter change. Most arteries and veins constrict after DEX administration. Vessel diameters from one rat were mostly dilated after DEX bolus administration (circles with X sign). Right panel – histogram of the vessel diameter ratios with a bin size of 0.01. Red and blue triangles indicate the median value in arteries (0.77) and veins (0.74), respectively. No significant difference was found between these medians (Mann–Whitney *U*-test, $P = 0.7546$). (D) Baseline CBF ratio is shown as a box plot ($n = 15$ rats). Median values of ISO levels from 15 rats before and after DEX administration were 1.3% (IQR, 0.1%) and 0.3% (IQR, 0.1%) respectively, and MABPs were 74.6 mmHg (IQR, 22.0 mmHg) and 113.4 mmHg (IQR, 29.9 mmHg), respectively (C, D).

$P = 0.0979$). No relationship was found between venous diameter and its change during stimulation ($r_{94} = -0.0687$, $P = 0.5104$).

Finally, the dynamic properties of CBF and vascular responses were examined by plotting normalised time courses of CBF along with arterial and venous diameter changes (Fig. 9C). The diameter changes in both arterial and venous vessels occurred as quickly as the CBF response. The time to return to baseline was observed first in CBF, then in arterial diameter, and finally in venous diameter. No post-stimulus undershoot was observed in CBF, arterial and venous diameter changes.

Discussion

DEX can elicit epileptic evoked responses

We have demonstrated that forelimb stimulation under continuous administration of DEX at 50 μg/kg/h for more than approximately 2 h elicited epileptic LFP responses with concomitant large increases in CBF (Fig. 2). Increasing the dose of DEX (150 μg/kg/h) did not prevent the development of the epileptic response. However, the addition of supplementary ISO (e.g. ~0.3%) suppressed the generation of the epileptic activity. Seizure activity associated with α_2-adrenergic receptor agonists (Mirski *et al.*, 1994; Miyazaki *et al.*, 1999; Rainger *et al.*, 2009) can be triggered by several factors. First, if O_2 availability is greatly decreased because of CBF reduction (as may happen with administration of DEX), hypoxic injuries could lead to seizures (Jensen *et al.*, 1991). However, SO_2 did not decrease to hypoxic levels under DEX with or without ISO (Table 2), and CBF appeared to be similar under DEX with or without ISO. Thus, hypoxia is probably not the mechanism causing the epileptic responses. Second, hyper-excitability induced by hyperglycemia (Schwechter *et al.*, 2003) could cause an evoked epileptic response. However, although both ISO and DEX can induce hyperglycemia (Nakadate *et al.*, 1980; DiTullio *et al.*, 1984; Morgan & Montague, 1985; Hikasa *et al.*, 1996; Kawano *et al.*, 2008), the data showed

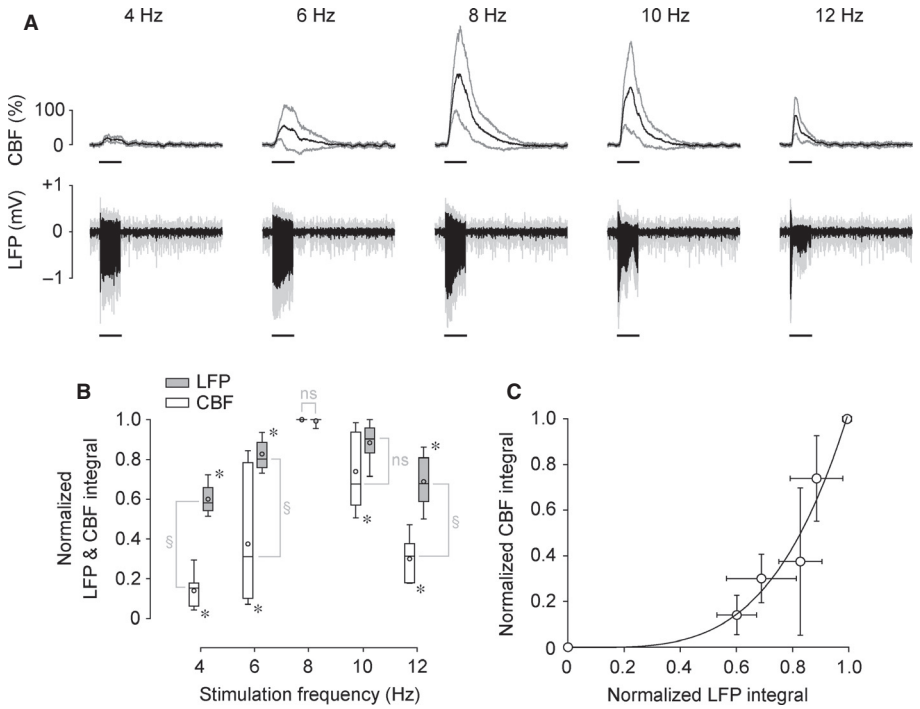

FIG. 7. CBF and LFP responses under DEX + ISO anesthesia are varied by stimulation frequency. (A) The time courses of CBF and LFP responses (mean and SDs) from seven rats are shown for five different stimulation frequencies. The horizontal bar under each trace indicates the 10-s stimulation period. (B) The integrals of LFP and CBF responses are plotted as a function of stimulation frequency. To reduce inter-animal variations, the integrals of these responses were calculated over the 10-s stimulation period for each stimulation frequency, and normalised by their maximum in each rat. Results are shown as box plots (open box, CBF; gray box, LFP). The LFP responses at 8 and 10 Hz were not significantly different (ns), but were significantly larger than the responses at other frequencies ($^*P < 0.05$). Similarly, the CBF response at 8 Hz was significantly larger than the responses at other frequencies ($^*P < 0.05$). The tuning curves of LFP and CBF responses differ significantly ($^{\S}P < 0.05$). Recording from seven rats started at a median time of 57.0 min (IQR, 26.3 min) after initial DEX administration, and continued for 5 min. Median values for ISO and MABP from seven rats were 0.4% (IQR, 0.1%) and 119.4 mmHg (IQR, 22.5 mmHg), respectively. (C) Relationship between mean LFP and mean CBF responses (circles in B). Error bars, +/– 1SD. A power law represented the data well (solid curve; CBF = $a\text{LFP}^b$), where $a = 1.03 \pm 0.09$ and $b = 3.84 \pm 0.70$ ($R^2 = 0.94$).

that only DEX elicited epileptic responses. Thus, hyperglycemia is probably not the primary cause of the epileptic response. Finally, perturbation of central adrenergic effects by DEX is most probably involved in seizure expression. As lesion of the locus coeruleus – the central adrenergic nucleus and the main target of DEX (Guo *et al.*, 1996) – causes seizures (Oishi & Suenaga, 1982), DEX administration may cause alternation of the net presynaptic inhibitory and postsynaptic excitatory balance (Samuels & Szabadi, 2008), eliciting evoked epileptic activity.

DEX supplemented with ISO prevents evoked epileptic responses

With supplementary ISO administration at levels > 0.1%, the evoked epileptic response was successfully suppressed in this study, possibly because of enhancement of the inhibitory action of GABA by ISO [for a review, see Campagna *et al.* (2003)]. As ISO at 0.1 minimum alveolar concentration (0.1–0.2%) produces hyperalgesia (Zhang *et al.*, 2000), DEX in combination with ISO at between 0.3% and 0.5% is recommended for rat forepaw model studies (e.g., Zhao *et al.*, 2012).

Although supplemental ISO administration with DEX effectively suppressed the development of evoked epileptic responses, it did not seem to stably extend the effects of DEX; that is, robust evoked CBF responses were usually obtained for up to at most 3 h under DEX + ISO anesthesia (Fig. 4). This duration matches the duration of the sedative effect of DEX; the effective hypnotic duration for DEX at 50 μg/kg/h (intraperitoneal, or intravenous MED at 100 μg/kg/h) is ~3 h (Doze *et al.*, 1989; Pawela *et al.*, 2009). Maintaining a stable sedative level is important for experimentation, as well as for obtaining robust responses. Increasing the blood concentration of DEX (Pawela *et al.*, 2009) would enhance the analgesic effect, but would not extend the sedative effect (Pertovaara *et al.*, 1991, 1994; Ansah *et al.*, 2000). The use of a higher ISO concentration could also help to enhance the analgesic effect rather than the sedative effect. Receptor desensitisation (Reid *et al.*, 1994; Hayashi *et al.*, 1995) or the competitive effect between α_1-adrenergic receptors and α_2-adrenergic receptors resulting from continuous DEX administration at a high dose can be related to the attenuation of the sedative effect. Although DEX is highly selective for presynaptic α_2-adrenergic receptors, inhibiting norepinephrine release from presynaptic sites, it also exerts an excitatory effect through postsynaptic α_1-adrenergic receptors when it exceeds a certain dosage (Doze *et al.*, 1989; Schwinn *et al.*, 1991), resulting in attenuation of α_2-mediated effects. Thus, the use of relatively low concentrations of DEX (with ISO or other anesthetics) can potentially extend the experimental duration. Recently, the combination of 30 μg/kg/h DEX and 0.25% ISO was able to maintain stable fMRI responses for up to ~4 h (Lu *et al.*, 2012).

DEX enhances slow-wave synchronous neural activity and evoked neural responses

The results show that LFP delta band power increased under DEX + ISO anesthesia, whereas beta and gamma band power decreased (Fig. 5), and this is consistent with previous electroen-

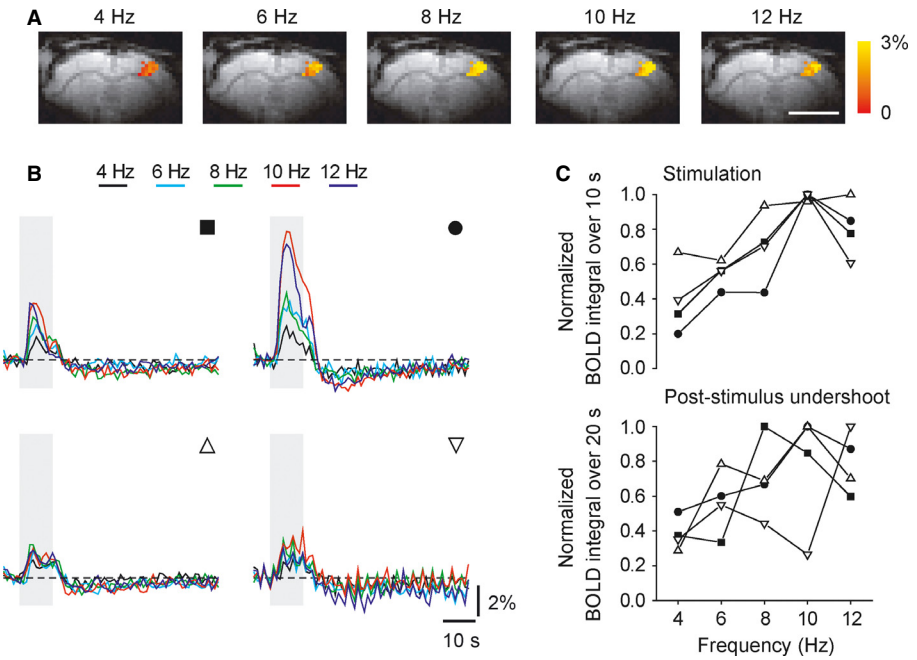

FIG. 8. Frequency-dependent BOLD fMRI response under DEX + ISO anesthesia. Five different frequencies were used. (A) BOLD fMRI maps of the response to left forepaw stimulation for five different frequencies in one rat are overlaid on echo-planar images. Scale bar: 5 mm. (B) BOLD fMRI time courses obtained from active pixels (e.g. color pixels in A). The gray vertical bar indicates a 10-s stimulation period. Upper panels identified by filled symbols were obtained from rats stimulated with a pulse width of 333 μs and a current of 2.4 mA; lower panels identified by open symbols were obtained from rats stimulated with a pulse width of 1 ms and a current of 1.5 mA. (C) Frequency tuning of positive BOLD responses during stimulation (upper panel) and post-stimulus undershoot (lower panel). Different symbols represent different rats (matched with B).

cephalography (EEG) findings (Farber *et al.*, 1997). Slow, synchronous, large-amplitude EEG are observed under anesthesia, whereas fast, desynchronous and low amplitude EEG are observed in a wakeful state (Bol *et al.*, 1997, 1999; Sloan, 1998). This synchronous and desynchronous switching can be attributed to changes in membrane potential states of neuronal cells. The membrane potential changes between up and down states under anesthesia, whereas it is persistently in an up-like state in a wakeful state (Constantinople & Bruno, 2011). Thalamic activity does not seem to be important for the persistent up-like state in the wakeful state, but the locus coeruleus seems to be critical (Constantinople & Bruno, 2011). As DEX directly inhibits norepinephrine release from the locus coeruleus, slow-wave fluctuations (i.e. bimodal up and down states) can become more prominent. The increase in the low-frequency band power may also enhance resting state functional connectivity under MED or DEX anesthesia (Pawela *et al.*, 2008, 2009; Zhao *et al.*, 2008; Williams *et al.*, 2010; Kalthoff *et al.*, 2011; Nasrallah *et al.*, 2012).

The results also show that the evoked LFP response under DEX + ISO was significantly larger than that under ISO only. A reduction in ISO concentration from 1.4% to < 0.5% is the likely reason for the enhancement of the LFP response (Banoub *et al.*, 2003). Also, DEX has a small effect on sensory-induced neural responses (Li *et al.*, 2003). The differential impacts of ISO and DEX on neural activity are not limited to evoked potential amplitudes. In the hippocampus, the BOLD response to identical stimuli depends on the previous stimulation history under MED, but not under ISO (Angenstein *et al.*, 2010; Krautwald & Angenstein, 2012). This suggests that ISO and MED interfere differently with hippocampal neural circuits (Angenstein *et al.*, 2010; Krautwald & Angenstein, 2012). These discrepancies can be explained by the fact that DEX does not involve the GABAergic system, but affects the neuromodulator epinephrine, unlike ISO. In other words, the neurovascular response under DEX should be different across brain regions [for example, see Fig. 5 in Nasrallah *et al.* (2012)], because the sensitivity to DEX varies across brain regions, depending on α_2-adrenergic receptor expression (Talley *et al.*, 1996).

DEX-induced vasoconstriction and CBF reduction

We showed that intravenous DEX at 50 μg/kg/h decreased baseline CBF and constricted both pial arteries and veins with supplemental ISO administration (Fig. 6). CBF reduction and pial vessel constriction induced by DEX have been well documented for various species. Whereas the cerebral vasoconstriction is mediated by direct agonist binding to α_2-adrenergic receptors on the cerebral vessels (Nakai *et al.*, 1986), the degree of vasoconstriction depends on the dose, the delivery method (topical vs. systemic), and anesthetics used prior to DEX administration (Karlsson *et al.*, 1990; Zornow *et al.*, 1990; Bari *et al.*, 1993; Fale *et al.*, 1994; McPherson *et al.*, 1994; Ishiyama *et al.*, 1995; Asano *et al.*, 1997; Ohata *et al.*, 1999; Iida *et al.*, 2006), as well as arterial carbon dioxide tension (Ganjoo *et al.*, 1998). For instance, the reductions in CBF and pial arterial diameter in hypocapnic rats were larger than those in normocapnic rats.

Although the behavior of pial vessels is expected to be generally similar to that of parenchymal vessels, their adrenergic innervations differ. Pial vessels are innervated by nerve terminals derived from peripheral superior cervical sympathetic ganglia, whereas parenchymal vessels (including capillaries) are innervated by nerve terminals derived from central adrenergic neurons within the brain, such as the locus coeruleus (Hartman *et al.*, 1972; Vaucher & Hamel, 1995;

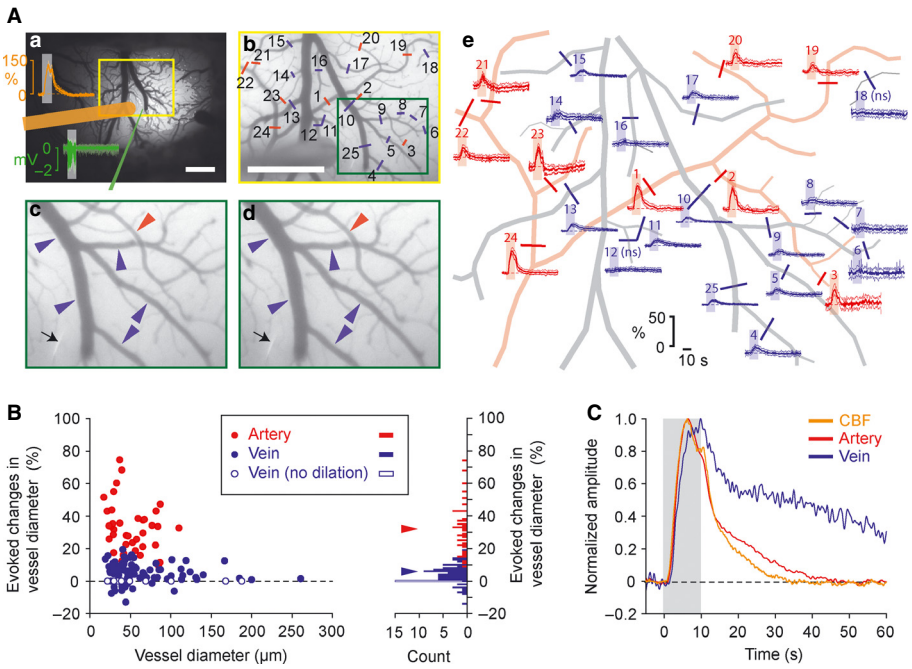

FIG. 9. Both pial arteries and veins dilate in response to forepaw stimulation under DEX + ISO anesthesia. Data from 11 rats were recorded at a median time of 77.0 min (IQR, 15.5 min) after initial DEX administration. Median values for ISO and MABP from 11 rats were 0.4% (IQR, 0.0%) and 100.9 mmHg (IQR, 0.9 mmHg), respectively. (A-a) Forepaw area mapped with flavoprotein autofluorescence signal overlaid on a cortical surface image. Mean (thick trace) and SD (pale trace) of CBF (orange trace) and LFP (green traces) responses during image acquisition for vessel diameter measurement and their measurement sites (orange bar, LDF probe; green line, microelectrode) are shown on the image. To record evoked changes in vessel diameters, images were taken from a yellow rectangular region every 100 ms. Scale: 1 mm. (A-b) Pre-stimulation image (average of five runs) from the yellow rectangular region shown in A-a. Evoked diameter changes were measured from labeled vessels (red bars on arteries, blue bars on veins), and their time courses are shown in A-e (see corresponding number). A green rectangular region is expanded in A-c and A-d for visual inspection of the vessel diameter changes. Scale bar: 1 mm. (A-c and A-d) Image at the onset of stimulation (c) and image at 10 s (d) after the onset of stimulation (average of five runs). Black arrows indicate the microelectrode used for LFP recording. Both arteries and veins dilate during stimulation (compare the vessel diameters indicated by the arrowheads (red, artery; blue, vein) between A-c and A-d). (A-e) Time courses of evoked diameter changes obtained from the vessels labeled in A-b (red, artery; blue, vein; mean and SD, thick and pale traces; horizontal broken line, baseline; gray bar, stimulation period). The major pial vessels seen in A-b were traced for better visualisation. ns, no significant diameter change. (B) Maximal evoked diameter changes during 10 s of stimulation for 38 arteries (red) and 94 veins (blue) measured from 11 rats. Median values of the number of arteries and veins measured per rat are 3 (IQR, 2.0) and 7 (IQR, 3.3), respectively. Left panel – relationship between evoked vessel diameter changes and basal vessel diameters. Solid circles indicate vessels with significant diameter change, and open blue circles indicate veins with no diameter change (n = 14). The horizontal broken line indicates no diameter change. No significant relationship was found between basal vessel diameter and diameter change in either arteries or veins. Right panel – histogram of the evoked diameter changes with a bin size of 1%. Red and blue triangles indicate medians of vessel dilation for arteries (32.2%) and veins (5.8%), respectively. (C) Normalised mean time courses of CBF (orange trace), arterial diameter (red trace) and venous diameter (blue trace) changes (averaged for 11 rats). The gray bar indicates the 10-s forepaw stimulation period. The venous diameter change occurred as quickly as the arterial diameter change, but the diameter returned to baseline more slowly than that of the artery. No post-stimulus undershoot was observed in mean CBF, arterial and venous diameter changes.

Paspalas & Papadopoulos, 1996; Cohen *et al.*, 1997). In the peripheral vasculature, vasodilation via sympathetic action and vasoconstriction mediated by smooth muscle receptors affected by DEX are known (for a review, see Kamibayashi & Maze, 2000). These different innervations might therefore explain the observation in one rat, although it is not clear why the dissociation between pial and parenchymal vessel diameter changes happened only in this rat (Fig. 6); that is, the dilation of pial vessels with DEX administration despite a decrease in baseline CBF, an indication of vasoconstriction in the parenchyma.

DEX administration yields robust CBF responses and rapid vasodilation

Evoked CBF responses under DEX + ISO were 3.7 times larger than those under ISO only, and the increase in LFP activity was 1.5 times larger. The large and rapid nature of evoked hemodynamic responses under DEX + ISO anesthesia (200–300% changes, Fig. 7; ~2% in BOLD, Fig. 8) is the most notable difference from the hemodynamic responses obtained under other anesthetics. This may be a result of the relatively high basal vascular tone induced by DEX (Fig. 6). Additionally, the effect of DEX on astrocyte activity may be considered, as astrocytes may be key mediators of neurovascular coupling (Zonta *et al.*, 2003; Takano *et al.*, 2006). Cortical astrocytes can be directly activated by somatosensory stimulation via the norepinephrine-dependent locus coeruleus pathway in addition to the general glutamate-dependent thalamocortical pathway (Bekar *et al.*, 2008). However, the locus coeruleus pathway is unlikely to have been involved in the present study, because it is activated only for pain stimulation. Thus, the enhancement of the hemodynamic response by DEX is not a result of activation of the additional pathway. The enhancement of energy metabolism in cortical astrocytes by DEX (Chen *et al.*, 2000) might have implications for the enhancement of the hemodynamic response. Further studies are necessary to understand the impact of the central adrenergic system on neurovascular coupling.

With other anesthetics, sensory stimulation evokes rapid vasodilation in pial arteries, followed by a delayed and slow increase in

venous CBV. This temporal character has been observed in α-chloralose-anesthetised rats during 40 s of forepaw stimulation (Zong *et al.*, 2012) and in wakeful mice during 30 s of vibrissa stimulation (Drew *et al.*, 2011). Earlier studies performed under ISO only (Kim *et al.*, 2007) showed that venous vessels did not dilate significantly during 10 s of stimulation. However, venous and arterial dilation were significant in response to 10 s of forepaw stimulation under DEX + ISO anesthesia, and the venous dilation was observed to be as fast as the arterial dilation, but took longer to return to baseline (Fig. 9). To our knowledge, dilation of pial veins and the increase in venous CBV in response to stimulation of such a short duration has not been found in animals anesthetised with isoflurane, α-chloralose, or urethane (Hillman *et al.*, 2007; Vazquez *et al.*, 2010a; Drew *et al.*, 2011). This discrepancy can be explained by the fact that DEX constricts pial veins as well as pial arteries, unlike other anesthetics. In addition, high basal vascular tone may make veins respond as fast as arteries. CBV increases resulting from venous dilation work to reduce the BOLD response, and a slow return to baseline in venous CBV (venous dilation) (Buxton *et al.*, 1998; Mandeville *et al.*, 1998, 1999) can account for the observed BOLD post-stimulus undershoot. Therefore, these findings suggest the opportunity to investigate the mechanism behind the BOLD response shape as a function of physiological parameters such as vascular tone.

Conclusion

The advantage of the combination of ~0.3% ISO and 50 μg/kg/h DEX is the suppression of epileptiform-like activity without changing the desired DEX effects for at least 3 h. Thus, DEX + ISO anesthesia will be beneficial for relatively short-term recoverable functional experiments, as the effects of DEX can be easily reversed with an α_2-adrenergic receptor antagonist, atipamezole. Our results could be useful not only for designing fMRI experiments with animal models under DEX sedation, but also for interpreting fMRI results obtained under this sedative.

Acknowledgements

We thank Ping Wang for his valuable assistance with the experiments. This work was supported by NIH grants R21-EB006571, K01-NS066131, R01-NS044589, and R01-EB003375.

Abbreviations

BOLD, blood oxygenation level-dependent; CBF, cerebral blood flow; CBV, cerebral blood volume; DEX, dexmedetomidine; EEG, electroencephalography; fMRI, functional magnetic resonance imaging; IQR, interquartile range; ISI, interstimulus interval; ISO, isoflurane; LDF, laser Doppler flowmetry; LFP, local field potential; MABP, mean arterial blood pressure; MED, medetomidine; MUA, multiple unit acitivity; Pco_2, arterial partial pressure of carbon dioxide; Po_2, arterial partial pressure of oxygen; ROI, region of interest; SD, standard deviation; So_2, arterial oxygen saturation level.

References

Airaksinen, A.M., Niskanen, J.P., Chamberlain, R., Huttunen, J.K., Nissinen, J., Garwood, M., Pitkanen, A. & Grohn, O. (2010) Simultaneous fMRI and local field potential measurements during epileptic seizures in medetomidine-sedated rats using raser pulse sequence. *Magn. Reson. Med.*, **64**, 1191–1199.

Angenstein, F., Krautwald, K. & Scheich, H. (2010) The current functional state of local neuronal circuits controls the magnitude of a BOLD response to incoming stimuli. *Neuroimage*, **50**, 1364–1375.

Ansah, O.B., Raekallio, M. & Vainio, O. (2000) Correlation between serum concentrations following continuous intravenous infusion of dexmedetomidine or medetomidine in cats and their sedative and analgesic effects. *J. Vet. Pharmacol. Ther.*, **23**, 1–8.

Asano, Y., Koehler, R.C., Kawaguchi, T. & McPherson, R.W. (1997) Pial arteriolar constriction to alpha 2-adrenergic agonist dexmedetomidine in the rat. *Am. J. Physiol.*, **272**, H2547–H2556.

Banoub, M., Tetzlaff, J.E. & Schubert, A. (2003) Pharmacologic and physiologic influences affecting sensory evoked potentials: implications for perioperative monitoring. *Anesthesiology*, **99**, 716–737.

Bari, F., Horvath, G. & Benedek, G. (1993) Dexmedetomidine-induced decrease in cerebral blood flow is attenuated by verapamil in rats: a laser Doppler study. *Can. J. Anaesth.*, **40**, 748–754.

Bekar, L.K., He, W. & Nedergaard, M. (2008) Locus coeruleus alpha-adrenergic-mediated activation of cortical astrocytes in vivo. *Cereb. Cortex*, **18**, 2789–2795.

Bekker, A. & Sturaitis, M.K. (2005) Dexmedetomidine for neurological surgery. *Neurosurgery*, **57**, 1–10; discussion 11–10.

Berwick, J., Martin, C., Martindale, J., Jones, M., Johnston, D., Zheng, Y., Redgrave, P. & Mayhew, J. (2002) Hemodynamic response in the unanesthetized rat: intrinsic optical imaging and spectroscopy of the barrel cortex. *J. Cereb. Blood Flow Metab.*, **22**, 670–679.

Bol, C., Danhof, M., Stanski, D.R. & Mandema, J.W. (1997) Pharmacokinetic–pharmacodynamic characterization of the cardiovascular, hypnotic, EEG and ventilatory responses to dexmedetomidine in the rat. *J. Pharmacol. Exp. Ther.*, **283**, 1051–1058.

Bol, C.J., Vogelaar, J.P. & Mandema, J.W. (1999) Anesthetic profile of dexmedetomidine identified by stimulus–response and continuous measurements in rats. *J. Pharmacol. Exp. Ther.*, **291**, 153–160.

Buxton, R.B., Wong, E.C. & Frank, L.R. (1998) Dynamics of blood flow and oxygenation changes during brain activation: the balloon model. *Magn. Reson. Med.*, **39**, 855–864.

Campagna, J.A., Miller, K.W. & Forman, S.A. (2003) Mechanisms of actions of inhaled anesthetics. *N. Engl. J. Med.*, **348**, 2110–2124.

Chen, Y., Zhao, Z., Code, W.E. & Hertz, L. (2000) A correlation between dexmedetomidine-induced biphasic increases in free cytosolic calcium concentration and energy metabolism in astrocytes. *Anesth. Analg.*, **91**, 353–357.

Cohen, Z., Molinatti, G. & Hamel, E. (1997) Astroglial and vascular interactions of noradrenaline terminals in the rat cerebral cortex. *J. Cereb. Blood Flow Metab.*, **17**, 894–904.

Constantinople, C.M. & Bruno, R.M. (2011) Effects and mechanisms of wakefulness on local cortical networks. *Neuron*, **69**, 1061–1068.

Correa-Sales, C., Rabin, B.C. & Maze, M. (1992) A hypnotic response to dexmedetomidine, an alpha 2 agonist, is mediated in the locus coeruleus in rats. *Anesthesiology*, **76**, 948–952.

DiTullio, N.W., Cieslinski, L., Matthews, W.D. & Storer, B. (1984) Mechanisms involved in the hyperglycemic response induced by clonidine and other alpha-2 adrenoceptor agonists. *J. Pharmacol. Exp. Ther.*, **228**, 168–173.

Doze, V.A., Chen, B.X. & Maze, M. (1989) Dexmedetomidine produces a hypnotic-anesthetic action in rats via activation of central alpha-2 adrenoceptors. *Anesthesiology*, **71**, 75–79.

Drew, P.J., Shih, A.Y. & Kleinfeld, D. (2011) Fluctuating and sensory-induced vasodynamics in rodent cortex extend arteriole capacity. *Proc. Natl. Acad. Sci. USA*, **108**, 8473–8478.

Fale, A., Kirsch, J.R. & McPherson, R.W. (1994) Alpha 2-adrenergic agonist effects on normocapnic and hypercapnic cerebral blood flow in the dog are anesthetic dependent. *Anesth. Analg.*, **79**, 892–898.

Farber, N.E., Poterack, K.A. & Schmeling, W.T. (1997) Dexmedetomidine and halothane produce similar alterations in electroencephalographic and electromyographic activity in cats. *Brain Res.*, **774**, 131–141.

Ganjoo, P., Farber, N.E., Hudetz, A., Smith, J.J., Samso, E., Kampine, J.P. & Schmeling, W.T. (1998) In vivo effects of dexmedetomidine on laser-Doppler flow and pial arteriolar diameter. *Anesthesiology*, **88**, 429–439.

Gsell, W., Burke, M., Wiedermann, D., Bonvento, G., Silva, A.C., Dauphin, F., Buhrle, C., Hoehn, M. & Schwindt, W. (2006) Differential effects of NMDA and AMPA glutamate receptors on functional magnetic resonance imaging signals and evoked neuronal activity during forepaw stimulation of the rat. *J. Neurosci.*, **26**, 8409–8416.

Guo, T.Z., Jiang, J.Y., Buttermann, A.E. & Maze, M. (1996) Dexmedetomidine injection into the locus ceruleus produces antinociception. *Anesthesiology*, **84**, 873–881.

Hartman, B.K., Zide, D. & Udenfriend, S. (1972) The use of dopamine-hydroxylase as a marker for the central noradrenergic nervous system in rat brain. *Proc. Natl. Acad. Sci. USA*, **69**, 2722–2726.

Hayashi, Y., Guo, T.Z. & Maze, M. (1995) Desensitization to the behavioral effects of alpha 2-adrenergic agonists in rats. *Anesthesiology*, **82**, 954–962.

Hikasa, Y., Kawanabe, H., Takase, K. & Ogasawara, S. (1996) Comparisons of sevoflurane, isoflurane, and halothane anesthesia in spontaneously breathing cats. *Vet. Surg.*, **25**, 234–243.

Hillman, E.M., Devor, A., Bouchard, M.B., Dunn, A.K., Krauss, G.W., Skoch, J., Bacskai, B.J., Dale, A.M. & Boas, D.A. (2007) Depth-resolved optical imaging and microscopy of vascular compartment dynamics during somatosensory stimulation. *Neuroimage*, **35**, 89–104.

Iida, H., Ohata, H., Iida, M., Watanabe, Y. & Dohi, S. (1998) Isoflurane and sevoflurane induce vasodilation of cerebral vessels via ATP-sensitive K^+ channel activation. *Anesthesiology*, **89**, 954–960.

Iida, H., Iida, M., Ohata, H., Michino, T. & Dohi, S. (2006) Effects of dexmedetomidine on cerebral circulation and systemic hemodynamics after cardiopulmonary resuscitation in dogs. *J. Anesth.*, **20**, 202–207.

Ishiyama, T., Dohi, S., Iida, H., Watanabe, Y. & Shimonaka, H. (1995) Mechanisms of dexmedetomidine-induced cerebrovascular effects in canine in vivo experiments. *Anesth. Analg.*, **81**, 1208–1215.

Jensen, F.E., Applegate, C.D., Holtzman, D., Belin, T.R. & Burchfiel, J.L. (1991) Epileptogenic effect of hypoxia in the immature rodent brain. *Ann. Neurol.*, **29**, 629–637.

Jevtovic-Todorovic, V., Todorovic, S.M., Mennerick, S., Powell, S., Dikranian, K., Benshoff, N., Zorumski, C.F. & Olney, J.W. (1998) Nitrous oxide (laughing gas) is an NMDA antagonist, neuroprotectant and neurotoxin. *Nat. Med.*, **4**, 460–463.

Kalso, E.A., Poyhia, R. & Rosenberg, P.H. (1991) Spinal antinociception by dexmedetomidine, a highly selective alpha 2-adrenergic agonist. *Pharmacol. Toxicol.*, **68**, 140–143.

Kalthoff, D., Seehafer, J.U., Po, C., Wiedermann, D. & Hoehn, M. (2011) Functional connectivity in the rat at 11.7T: impact of physiological noise in resting state fMRI. *Neuroimage*, **54**, 2828–2839.

Kamibayashi, T. & Maze, M. (2000) Clinical uses of alpha2-adrenergic agonists. *Anesthesiology*, **93**, 1345–1349.

Karlsson, B.R., Forsman, M., Roald, O.K., Heier, M.S. & Steen, P.A. (1990) Effect of dexmedetomidine, a selective and potent alpha 2-agonist, on cerebral blood flow and oxygen consumption during halothane anesthesia in dogs. *Anesth. Analg.*, **71**, 125–129.

Kawano, T., Tanaka, K., Mawatari, K., Oshita, S., Takahashi, A. & Nakaya, Y. (2008) Hyperglycemia impairs isoflurane-induced adenosine triphosphate-sensitive potassium channel activation in vascular smooth muscle cells. *Anesth. Analg.*, **106**, 858–864.

Kim, T., Hendrich, K.S., Masamoto, K. & Kim, S.G. (2007) Arterial versus total blood volume changes during neural activity-induced cerebral blood flow change: implication for BOLD fMRI. *J. Cereb. Blood Flow Metab.*, **27**, 1235–1247.

Kim, T., Masamoto, K., Fukuda, M., Vazquez, A. & Kim, S.G. (2010) Frequency-dependent neural activity, CBF, and BOLD fMRI to somatosensory stimuli in isoflurane-anesthetized rats. *Neuroimage*, **52**, 224–233.

Krautwald, K. & Angenstein, F. (2012) Low frequency stimulation of the perforant pathway generates anesthesia-specific variations in neural activity and BOLD responses in the rat dentate gyrus. *J. Cereb. Blood Flow Metab.*, **32**, 291–305.

Li, B.H., Lohmann, J.S., Schuler, H.G. & Cronin, A.J. (2003) Preservation of the cortical somatosensory-evoked potential during dexmedetomidine infusion in rats. *Anesth. Analg.*, **96**, 1155–1160.

Lu, H., Zou, Q., Gu, H., Raichle, M.E., Stein, E.A. & Yang, Y. (2012) Rat brains also have a default mode network. *Proc. Natl. Acad. Sci. USA*, **109**, 3979–3984.

MacDonald, E., Scheinin, M., Scheinin, H. & Virtanen, R. (1991) Comparison of the behavioral and neurochemical effects of the two optical enantiomers of medetomidine, a selective alpha-2-adrenoceptor agonist. *J. Pharmacol. Exp. Ther.*, **259**, 848–854.

Mandeville, J.B., Marota, J.J., Kosofsky, B.E., Keltner, J.R., Weissleder, R., Rosen, B.R. & Weisskoff, R.M. (1998) Dynamic functional imaging of relative cerebral blood volume during rat forepaw stimulation. *Magn. Reson. Med.*, **39**, 615–624.

Mandeville, J.B., Marota, J.J., Ayata, C., Zaharchuk, G., Moskowitz, M.A., Rosen, B.R. & Weisskoff, R.M. (1999) Evidence of a cerebrovascular postarteriole windkessel with delayed compliance. *J. Cereb. Blood Flow Metab.*, **19**, 679–689.

Martin, C., Martindale, J., Berwick, J. & Mayhew, J. (2006) Investigating neural–hemodynamic coupling and the hemodynamic response function in the awake rat. *Neuroimage*, **32**, 33–48.

Masamoto, K., Kim, T., Fukuda, M., Wang, P. & Kim, S.G. (2007) Relationship between neural, vascular, and BOLD signals in isoflurane-anesthetized rat somatosensory cortex. *Cereb. Cortex*, **17**, 942–950.

Masamoto, K., Fukuda, M., Vazquez, A. & Kim, S.G. (2009) Dose-dependent effect of isoflurane on neurovascular coupling in rat cerebral cortex. *Eur. J. Neurosci.*, **30**, 242–250.

McPherson, R.W., Kirsch, J.R. & Traystman, R.J. (1994) Inhibition of nitric oxide synthase does not affect alpha 2-adrenergic-mediated cerebral vasoconstriction. *Anesth. Analg.*, **78**, 67–72.

Mennerick, S., Jevtovic-Todorovic, V., Todorovic, S.M., Shen, W., Olney, J. W. & Zorumski, C.F. (1998) Effect of nitrous oxide on excitatory and inhibitory synaptic transmission in hippocampal cultures. *J. Neurosci.*, **18**, 9716–9726.

Mirski, M.A., Rossell, L.A., McPherson, R.W. & Traystman, R.J. (1994) Dexmedetomidine decreases seizure threshold in a rat model of experimental generalized epilepsy. *Anesthesiology*, **81**, 1422–1428.

Miyazaki, Y., Adachi, T., Kurata, J., Utsumi, J., Shichino, T. & Segawa, H. (1999) Dexmedetomidine reduces seizure threshold during enflurane anaesthesia in cats. *Br. J. Anaesth.*, **82**, 935–937.

Morgan, N.G. & Montague, W. (1985) Studies on the mechanism of inhibition of glucose-stimulated insulin secretion by noradrenaline in rat islets of Langerhans. *Biochem. J.*, **226**, 571–576.

Nakadate, T., Nakaki, T., Muraki, T. & Kato, R. (1980) Adrenergic regulation of blood glucose levels: possible involvement of postsynaptic alpha-2 type adrenergic receptors regulating insulin release. *J. Pharmacol. Exp. Ther.*, **215**, 226–230.

Nakai, K., Itakura, T., Naka, Y., Nakakita, K., Kamei, I., Imai, H., Yokote, H. & Komai, N. (1986) The distribution of adrenergic receptors in cerebral blood vessels: an autoradiographic study. *Brain Res.*, **381**, 148–152.

Nasrallah, F.A., Tan, J. & Chuang, K.H. (2012) Pharmacological modulation of functional connectivity: alpha2-adrenergic receptor agonist alters synchrony but not neural activation. *Neuroimage*, **60**, 436–446.

Norup Nielsen, A. & Lauritzen, M. (2001) Coupling and uncoupling of activity-dependent increases of neuronal activity and blood flow in rat somatosensory cortex. *J. Physiol.*, **533**, 773–785.

Ohata, H., Iida, H., Dohi, S. & Watanabe, Y. (1999) Intravenous dexmedetomidine inhibits cerebrovascular dilation induced by isoflurane and sevoflurane in dogs. *Anesth. Analg.*, **89**, 370–377.

Oishi, R. & Suenaga, N. (1982) The role of the locus coeruleus in regulation of seizure susceptibility in rats. *Jpn. J. Pharmacol.*, **32**, 1075–1081.

Paspalas, C.D. & Papadopoulos, G.C. (1996) Ultrastructural relationships between noradrenergic nerve fibers and non-neuronal elements in the rat cerebral cortex. *Glia*, **17**, 133–146.

Pawela, C.P., Biswal, B.B., Cho, Y.R., Kao, D.S., Li, R., Jones, S.R., Schulte, M.L., Matloub, H.S., Hudetz, A.G. & Hyde, J.S. (2008) Resting-state functional connectivity of the rat brain. *Magn. Reson. Med.*, **59**, 1021–1029.

Pawela, C.P., Biswal, B.B., Hudetz, A.G., Schulte, M.L., Li, R., Jones, S.R., Cho, Y.R., Matloub, H.S. & Hyde, J.S. (2009) A protocol for use of medetomidine anesthesia in rats for extended studies using task-induced BOLD contrast and resting-state functional connectivity. *Neuroimage*, **46**, 1137–1147.

Pertovaara, A., Kauppila, T., Jyvasjarvi, E. & Kalso, E. (1991) Involvement of supraspinal and spinal segmental alpha-2-adrenergic mechanisms in the medetomidine-induced antinociception. *Neuroscience*, **44**, 705–714.

Pertovaara, A., Hamalainen, M.M., Kauppila, T., Mecke, E. & Carlson, S. (1994) Dissociation of the alpha 2-adrenergic antinociception from sedation following microinjection of medetomidine into the locus coeruleus in rats. *Pain*, **57**, 207–215.

Rainger, J., Baxter, C., Vogelnest, L. & Dart, C. (2009) Seizures during medetomindine sedation and local anaesthesia in two dogs undergoing skin biopsy. *Aust. Vet. J.*, **87**, 188–192.

Ramos-Cabrer, P., Weber, R., Wiedermann, D. & Hoehn, M. (2005) Continuous noninvasive monitoring of transcutaneous blood gases for a stable and persistent BOLD contrast in fMRI studies in the rat. *NMR Biomed.*, **18**, 440–446.

Reid, K., Hayashi, Y., Guo, T.Z., Correa-Sales, C., Nacif-Coelho, C. & Maze, M. (1994) Chronic administration of an alpha 2 adrenergic agonist desensitizes rats to the anesthetic effects of dexmedetomidine. *Pharmacol. Biochem. Behav.*, **47**, 171–175.

Samuels, E.R. & Szabadi, E. (2008) Functional neuroanatomy of the noradrenergic locus coeruleus: its roles in the regulation of arousal and autonomic function part II: physiological and pharmacological manipulations and pathological alterations of locus coeruleus activity in humans. *Curr. Neuropharmacol.*, **6**, 254–285.

Savola, J.M. & Virtanen, R. (1991) Central alpha 2-adrenoceptors are highly stereoselective for dexmedetomidine, the dextro enantiomer of medetomidine. *Eur. J. Pharmacol.*, **195**, 193–199.

Savola, M.K., MacIver, M.B., Doze, V.A., Kendig, J.J. & Maze, M. (1991) The alpha 2-adrenoceptor agonist dexmedetomidine increases the apparent

potency of the volatile anesthetic isoflurane in rats in vivo and in hippocampal slice in vitro. *Brain Res.*, **548**, 23–28.
Scheinin, H., Virtanen, R., MacDonald, E., Lammintausta, R. & Scheinin, M. (1989) Medetomidine – a novel alpha 2-adrenoceptor agonist: a review of its pharmacodynamic effects. *Prog. Neuropsychopharmacol. Biol. Psychiatry*, **13**, 635–651.
Schmeling, W.T., Kampine, J.P., Roerig, D.L. & Warltier, D.C. (1991) The effects of the stereoisomers of the alpha 2-adrenergic agonist medetomidine on systemic and coronary hemodynamics in conscious dogs. *Anesthesiology*, **75**, 499–511.
Schwechter, E.M., Veliskova, J. & Velisek, L. (2003) Correlation between extracellular glucose and seizure susceptibility in adult rats. *Ann. Neurol.*, **53**, 91–101.
Schwinn, D.A., Correa-Sales, C., Page, S.O. & Maze, M. (1991) Functional effects of activation of alpha-1 adrenoceptors by dexmedetomidine: in vivo and in vitro studies. *J. Pharmacol. Exp. Ther.*, **259**, 1147–1152.
Seehafer, J.U., Kalthoff, D., Farr, T.D., Wiedermann, D. & Hoehn, M. (2010) No increase of the blood oxygenation level-dependent functional magnetic resonance imaging signal with higher field strength: implications for brain activation studies. *J. Neurosci.*, **30**, 5234–5241.
Segal, I.S., Vickery, R.G., Walton, J.K., Doze, V.A. & Maze, M. (1988) Dexmedetomidine diminishes halothane anesthetic requirements in rats through a postsynaptic alpha 2 adrenergic receptor. *Anesthesiology*, **69**, 818–823.
Sinclair, M.D. (2003) A review of the physiological effects of alpha2-agonists related to the clinical use of medetomidine in small animal practice. *Can. Vet. J.*, **44**, 885–897.
Sloan, T., Sloan, H. & Rogers, J. (2010) Nitrous oxide and isoflurane are synergistic with respect to amplitude and latency effects on sensory evoked potentials. *J. Clin. Monit. Comput.*, **24**, 113–123.
Sloan, T.B. (1998) Anesthetic effects on electrophysiologic recordings. *J. Clin. Neurophysiol.*, **15**, 217–226.
Takano, T., Tian, G.F., Peng, W., Lou, N., Libionka, W., Han, X. & Nedergaard, M. (2006) Astrocyte-mediated control of cerebral blood flow. *Nat. Neurosci.*, **9**, 260–267.
Talley, E.M., Rosin, D.L., Lee, A., Guyenet, P.G. & Lynch, K.R. (1996) Distribution of alpha 2A-adrenergic receptor-like immunoreactivity in the rat central nervous system. *J. Comp. Neurol.*, **372**, 111–134.
Van Camp, N., Verhoye, M., De Zeeuw, C.I. & Van der Linden, A. (2006) Light stimulus frequency dependence of activity in the rat visual system as studied with high-resolution BOLD fMRI. *J. Neurophysiol.*, **95**, 3164–3170.
Vaucher, E. & Hamel, E. (1995) Cholinergic basal forebrain neurons project to cortical microvessels in the rat: electron microscopic study with anterogradely transported *Phaseolus vulgaris* leucoagglutinin and choline acetyltransferase immunocytochemistry. *J. Neurosci.*, **15**, 7427–7441.
Vazquez, A.L., Fukuda, M., Tasker, M.L., Masamoto, K. & Kim, S.G. (2010a) Changes in cerebral arterial, tissue and venous oxygenation with evoked neural stimulation: implications for hemoglobin-based functional neuroimaging. *J. Cereb. Blood Flow Metab.*, **30**, 428–439.
Vazquez, A.L., Masamoto, K., Fukuda, M. & Kim, S.G. (2010b) Cerebral oxygen delivery and consumption during evoked neural activity. *Front. Neuroenergetics*, **2**, 11.
Vazquez, A.L., Fukuda, M. & Kim, S.G. (2012) Evolution of the dynamic changes in functional cerebral oxidative metabolism from tissue mitochondria to blood oxygen. *J. Cereb. Blood Flow Metab.*, **32**, 745–758.
Vickery, R.G. & Maze, M. (1989) Action of the stereoisomers of medetomidine, in halothane-anesthetized dogs. *Acta Vet. Scand. Suppl.*, **85**, 71–76.
Weber, R., Ramos-Cabrer, P., Wiedermann, D., van Camp, N. & Hoehn, M. (2006) A fully noninvasive and robust experimental protocol for longitudinal fMRI studies in the rat. *Neuroimage*, **29**, 1303–1310.
Weber, R., Ramos-Cabrer, P., Justicia, C., Wiedermann, D., Strecker, C., Sprenger, C. & Hoehn, M. (2008) Early prediction of functional recovery after experimental stroke: functional magnetic resonance imaging, electrophysiology, and behavioral testing in rats. *J. Neurosci.*, **28**, 1022–1029.
White, P.F., Johnston, R.R. & Eger, E.I. 2nd (1974) Determination of anesthetic requirement in rats. *Anesthesiology*, **40**, 52–57.
Williams, K.A., Magnuson, M., Majeed, W., LaConte, S.M., Peltier, S.J., Hu, X. & Keilholz, S.D. (2010) Comparison of alpha-chloralose, medetomidine and isoflurane anesthesia for functional connectivity mapping in the rat. *Magn. Reson. Imaging*, **28**, 995–1003.
Zhang, Y., Eger, E.I. 2nd, Dutton, R.C. & Sonner, J.M. (2000) Inhaled anesthetics have hyperalgesic effects at 0.1 minimum alveolar anesthetic concentration. *Anesth. Analg.*, **91**, 462–466.
Zhao, F., Zhao, T., Zhou, L., Wu, Q. & Hu, X. (2008) BOLD study of stimulation-induced neural activity and resting-state connectivity in medetomidine-sedated rat. *Neuroimage*, **39**, 248–260.
Zhao, F., Welsh, D., Williams, M., Coimbra, A., Urban, M.O., Hargreaves, R., Evelhoch, J. & Williams, D.S. (2012) fMRI of pain processing in the brain: a within-animal comparative study of BOLD vs. CBV and noxious electrical vs. noxious mechanical stimulation in rat. *Neuroimage*, **59**, 1168–1179.
Zong, X., Kim, T. & Kim, S.G. (2012) Contributions of dynamic venous blood volume versus oxygenation level changes to BOLD fMRI. *Neuroimage*, **60**, 2238–2246.
Zonta, M., Angulo, M.C., Gobbo, S., Rosengarten, B., Hossmann, K.A., Pozzan, T. & Carmignoto, G. (2003) Neuron-to-astrocyte signaling is central to the dynamic control of brain microcirculation. *Nat. Neurosci.*, **6**, 43–50.
Zornow, M.H., Fleischer, J.E., Scheller, M.S., Nakakimura, K. & Drummond, J.C. (1990) Dexmedetomidine, an alpha 2-adrenergic agonist, decreases cerebral blood flow in the isoflurane-anesthetized dog. *Anesth. Analg.*, **70**, 624–630.